Kyoto University

A Level Set-Based Topology Optimization incorporating concept of the phase-field method

(フェーズフィールド法の考え方を用いたレベルセット法に基づくトポロジー最適化)

by

Takayuki Yamada

A Dissertation Submitted in partial fulfillment
of the requirements for the Degree of Doctor of Philosophy

in the

Graduate School of Engineering
Department of Aeronautics and Astronautics

September 2010

KYOTO UNIVERSITY

Abstract

Graduate School of Engineering

Department of Aeronautics and Astronautics

Doctor of Enginnering

by Takayuki Yamada

This doctoral thesis presents a new level set-based topology optimization method, which can adjust the geometrical complexity of obtained optimal configurations, that uses a fictitious interface energy based on the concept of the phase field model. The novel aspects of this method are the incorporation of level set-based boundary expressions and the fictitious interface energy in the topology optimization problem, and the replacement of the original topology optimization problem with a procedure to solve a reaction-diffusion equation.

First, background information concerning the structural optimization field is given, and the features of level set-based optimization methods are explained. The history of how I developed the new level set-based topology optimization method is discussed, and the objective of this thesis is described.

Next, a topology optimization problem is formulated based on level set-based structural boundary expressions, and the method of regularizing the optimization problem by introducing a fictitious interface energy is explained. The reaction-diffusion equation that updates the level set function is derived and an optimization algorithm is then constructed. The optimization algorithm uses the Finite Element Method and Finite Difference Method to solve the equilibrium equations and the reaction-diffusion equation when updating the level set function.

A number of optimum design examples are presented, namely, minimum mean compliance problems, the optimum design of compliant mechanisms, lowest eigenfrequency maximization problems, and thermal problems, to demonstrate the versatility and effectiveness of the presented topology optimization method.

The thesis ends with a personal statement concerning my journey up to the present, and goals for the future.

Acknowledgements

I would like to take this opportunity to thank the many people who have contributed to the realization of my doctorate dissertation. First, I would like to thank Professor Masataka Yoshimura, Professor Shinji Nishiwaki and Professor Kazuhiro Izui, who have given me invaluable support and advice throughout the course of my Masters and Doctorate research.

I am especially grateful to Professor Shinji Nishiwaki, who has provided continuous encouragement and support, given me the freedom to develop my own ideas and the chance to collaborate with various professors, including foreign researchers. Under his aegis, I have had a number of research papers published, have been awarded prizes such as the JSME best paper award for 2009, and have been able to exploit my time at Kyoto University doing research in my chosen field.

In addition, I would like to thank all the members of the Yoshimura and Nishiwaki Labs: Dr. Kaeseok Choi, Dr. Yoel Tenne, Dr. Ranjan Kumar, Dr. Atsurou Iga, Mr. Ryuhei Nishimura, Dr. Shintaro Yamasaki, Dr. Kenji Doi, Mr. Jacob Andkjar, Mr. Shunsuke Ikeuchi, Mr. Yoshiyuki Chuzyo, Mr. Yu Yoshimura, Mr. Masatoshi Manabe, Ms. Takayo Kotani, Mr. Masaki Otomori, Mr. Naotaka Uchida, Mr. Keiichi Noda, Mr. Shin Kikuchi, Mr. Kiyoshi Yokota, Mr. Yuji Okamoto, Ms. Eri Kujiraoka, Mr. Yushuke Soda, Mr. Akihisa Tozaki, Mr. Keisuke Mizushiri, Mr. Keiji Yamaguchi, Mr. Hidetsugu Wada, Mr. Ippei Kawai, Mr. Masaharu Kizu, Mr. Yutaka Saito, Mr. Daisuke Hanatani, Mr. Lim Yi Kang, Mr. Takakazu Yoshifuji, Mr. Yutaka Murakumo and Mr. Shouta Tsukamoto.

I would also like to thank Professor Takaji Inamuro, Professor Taku Ohwada and Professor Hiroshi Sugimoto for their support and advice throughout the course of my undergraduate research at Kyoto University. My joining the Inamuro Lab exposed me to sound academic practices and helped me develop a logical way of thinking, experiences that became the foundation of my doctorate research. I extend my gratitude to all member of the Inamuro Lab, Dr. Syugo Yasuda, Mr. Bunpei Sakakibara, Mr. Joji Tomiyasu, Mr. Wataru Sato, Mr. Hiroshi Hayashi, Mr. Kenya Moriuchi and Mr. Shigeru Kawakami.

I am extremely grateful to the many Professors who helped me during collaborative research. Due to their energy and generosity, I was exposed to a variety of disciplines and avenues of research, such as fuel cells, engineering for synthetic nanosystems, and reliability-based optimization. Thus, I offer my heartfelt thanks to:

Professor Hideo Yoshida, Professor Hiroshi Iwai and Mr. Atsushi Kuroyanagi of Kyoto University for collaborating in research concerning the optimum design of cathode/electrolyte interfaces for SOFC (solid oxide fuel cells).

Professor Osamu Tabata and Mr. Masashi Sato of Kyoto University for collaborating in research concerning optimum design methods for micro-devices.

Professor Alejandro R. Diaz and Ms. Kazuko Fuchi of Michigan State University for collaborating in research on topology optimization, and their unstinting hospitality during my stay at Lansing, Michigan.

Professor Seungjae Min and Mr. Sunghoon Lim of Hanyang University for collaborating in research on topology optimization applied to magnetic actuators.

Professor Kenjiro Terada and Professor Mao Kurumatani of Tohoku University for collaborating in research on a topology optimization method incorporating the Finite Cover Method.

Professor Nozomu Kogiso and Mr. Yutaka Hirano of Osaka Prefecture University for collaborating in research on reliability-based optimization methods.

Professor Gakuji Nagai and Mr. Takanori Kato of Gifu University for collaborating in research on the optimum design of magnetostrictive actuators.

Professor Shintaro Yamasaki, Professor Masakazu Kobayashi and Professor Akihiro Takezawa, members of a study meeting concerning level set-based optimization methods, for their stimulating discussions and deep insights.
Dr. Tsuyoshi Nomura of Toyota Central R&D Labs, Inc., for his generous assistance in my research and his deep understanding of topology optimization methods.
Dr. Shinichi Maruyama and Dr. Takashi Yamamoto of Nissan Motor Co., Ltd., for collaborating in research on applying a level set-based optimum design method to automotive body structure designs.

I would also like to thank Mr. John Goodman for his help in editing the papers I have written in English.

I sincerely appreciate the support received from the following:

- The Moriyasu Graduate School Fellowship Fund.
- The Kyoto University Foundation, Grants for Researchers Attending International Meetings.
- The NEC C&C Foundation, Grants for Researchers Attending International Conferences.
- The Japan Society for the Promotion of Science, Research Fellowship for Young Scientists. (JSPS Fellows, DC).

And finally, I am most grateful to my parents and my sister, for their encouragement and support throughout my life.

Takayuki Yamada

Kyoto, April, 2010

To my parents and my sister

To my friends

Contents

List of Figures

Chapter 1

Introduction

1.1 Structural optimization

Structural optimization has been successfully used in many industries such as automotive industries. Structural optimization can be classified into sizing[1, 2], shape[3, 4, 5, 6, 7] and topology optimization [8, 9, 10, 11], the last offering the most potential for exploring ideal and optimized structures. As the most flexible structural optimization, topology optimization allows changes not only in shape but also in the topology of target structures, and is potentially the most useful type of optimization when seeking to create high-performance structural configurations. Topology optimization has been extensively applied to a variety of structural optimization problems such as the stiffness maximization problem [8, 12], vibration problems [13, 14, 15], optimum design problems for compliant mechanisms [16, 17], and thermal problems [18, 19, 20], after Bensdøe and Kikuchi [8] first proposed the so-called Homogenization Design Method. The basic concepts of topology optimization are (1) the extension of a design domain to a fixed design domain, and (2) replacement of the optimization problem with material distribution problem, using the characteristic function [21]. A homogenization method [8, 11, 22, 23, 24] is utilized to deal with the extreme discontinuity of material distribution and to provide the material properties viewed in a global sense as homogenized properties. The Homogenization Design Method (HDM) has been applied to a variety of design problems. The density approach [25], also called the SIMP (Solid Isotropic Material with Penalization) method [26, 27], is another currently used topology optimization method, the basic idea of which is the use of a fictitious isotropic material whose elasticity tensor is assumed to be a function of penalized material density, represented by an exponent parameter. Bendsøe and Sigmund [28] asserted the validity of the SIMP method in view of the mechanics of composite materials. The phase field model based on the theory of phase transitions [29, 30, 31, 32] is also used as another approach toward regularizing topology optimization problems and penalizing material density [33, 34, 35, 36, 37, 38]. In these methods, by adding a Cahn-Hilliard-type penalization functional [29] to an objective functional, the topology optimization problem is regularized and the material density penalized. The phase field model utilized in certain structural optimization methods employs a regularization technique based on the imposition of some degree of shape smoothness, but these methods also yield optimal configurations that include grayscales.

In addition to the above conventional approaches, a different type of method, called the evolutionary structural optimization (ESO) method [15, 39], has been proposed. In this method, the design domain is discretized using a finite element mesh and unnecessary elements are removed based on heuristic criteria so that the optimal configuration is ultimately obtained as an optimal subset of finite elements.

Unfortunately, the conventional topology optimization methods tend to suffer from numerical instability problems [40, 41], such as mesh dependency, checkerboard patterns and grayscales. Several methods have been proposed to mitigate these instability problems, such as the use of high-order finite elements [40] and filtering schemes [41]. Although various filtering schemes are currently used, they crucially depend on artificial parameters that lack rational guidelines for determining appropriate *a priori* parameter values. Additionally, optimal configurations can include highly complex geometrical structures that are inappropriate from an engineering and manufacturing standpoint. Although a number of geometrical constraint methods for topology optimization methods have been proposed, such as the perimeter control method [42] and member size control method [43, 44], the parameters and the complexity of obtained optimal configurations are not uniquely linked. Furthermore, geometrical constraint methods often make the optimization procedure unstable. Thus, a geometric constraint method in which the complexity of the optimal configuration can be set uniquely, and which also maintains stability in the optimization procedure, has yet to be proposed.

1.2 Level set method

A different approach is used in level set-based structural optimization methods that have been proposed as a new type of structural optimization method. Such methods implicitly represent target structural configurations using the iso-surface of the level set function, which is a scalar function, and the outlines of target structures are changed by updating the level set function during the optimization process. The level set method was originally proposed by Osher and Sethian [45] as a versatile method to implicitly represent evolutional interfaces in an Eulerian coordinate system. The evolution of the boundaries with respect to time is tracked by solving the so-called Hamilton-Jacobi partial differential equation, with an appropriate normal velocity that is the moving boundary velocity normal to the interface. Level set methods are potentially useful in a variety of applications, including fluid mechanics [46, 47, 48], phase transitions [49], image processing [50, 51, 52] and solid modeling in CAD [53].

In level set-based structural optimization methods, complex shape and topological changes can be handled and the obtained optimal structures are free from grayscales, since the structural boundaries are represented as the iso-surface of the level set function. Although these relatively new structural optimization methods overcome the problems of checkerboard patterns and grayscales, mesh dependencies have yet to be eliminated.

1.3 Level set-based structural optimization

Sethian and Wiegmann [54] first proposed a level set-based structural optimization method where the level set function is updated using an ad hoc method based on the Von Mises stress. Osher and Santosa [55] proposed a structural optimization method where the shape sensitivity is used as the normal velocity, and the structural optimization is performed by solving the level set equation using the upwind scheme. This proposed method was applied to eigen-frequency problems for an inhomogeneous drum using a two-phase optimization of the membrane where the mass density assumes two different values, while the elasticity tensor is constant over the entire domain.

Belytschko *et al.* [56] proposed a topology optimization using an implicit function to represent structural boundaries and their method allows topological changes by introducing the concept of an active zone where the material properties such as Young's modulus are smoothly distributed. Wang *et al.* [57] proposed a shape optimization method based on the level set method where the level set function is updated using the Hamilton-Jacobi equation, also called the level set equation, based on the shape sensitivities and the proposed method was applied to the minimum mean compliance problem. Wang and Wang [58] extended this method to a multi-material optimal design problem using a "color" level set method where m level set functions are used to represent 2^m different material phases. Allaire *et al.* [59] independently proposed a level set-based shape optimization method where the level set function is updated using smoothed shape sensitivities that are mapped to the design domain using a smoothing technique. A simple "ersatz material" approach was employed to compute the displacement field of the structure, and optimal configurations were obtained for the minimum compliance problem for both structures composed of linear elastic and non-linear hyperelastic material, and compliant mechanism structural design problems. Allaire and Jouve [60] also extended their method to lowest eigen-frequency maximization problems and minimum compliance problems having multiple loads. Leitao and Scherzer [61] also proposed a shape optimization method using the level set-based structural boundary expressions. In this method, Tikhonov regularization method are introduced for regularizing the optimization problem.

Recently, numerous extensions of the level set-based method have been presented, such as the use of different expressions [62], the use of a specific numerical method such as meshless methods [63], the use of mathematical approaches in the optimization scheme [64], and other applications, such as optimum design of multiphysics actuators and thermo-elastic problems [65, 66, 67, 68, 69].

The above level set-based structural optimization methods can be said to be a type of shape optimization method, since the shape boundaries of target structures are evolved from an initial configuration by updating the level set equation using shape sensitivities. Therefore, topological changes that increase the number of holes in the material domain are not permitted, although topological changes that decrease the number of holes are allowed. As a result, the obtained optimal configurations strongly depend on the given initial configuration. To provide for the possibility of topological changes, Allaire *et al.* [70] introduced the bubble method [71] to a level set-based shape optimization method using topological derivatives [72, 73, 74]. In Allaire's method [70], structural boundaries are updated based on smoothed shape sensitivities using the level set equation and holes are introduced during the optimization process. Appropriate optimal configurations were obtained using several different initial configurations, however parameter setting with respect to the introduction of holes during the optimization process was difficult and potentially affected the obtained optimal configurations.

Wang *et al.* [75] proposed an extended level set method for a topology optimization method based on one of their previously proposed methods [57]. In their method [75], an extended velocity which has a non zero value in the material domain is introduced and the level set function is not reinitialized to maintain the property of a signed distance function. Topological changes including the introduction of holes in a material domain are therefore allowed, however the extended velocity cannot be logically determined, since the level set equation is derived based the boundary advection concept. As a result, it is difficult to define appropriate extended velocities and the definition of the extension velocities in large measure determines the shape of the obtained optimal structures.

In level set-based shape optimization methods using the Hamilton-Jacobi equation, the level set function must be re-initialized to maintain the signed distance characteristic of the function. This re-initialization operation [76, 53, 46] is not an easy task, and a number of level set-based topology optimization methods that do not depend on boundary advection concepts have been proposed recently. Wang and Wang [77] proposed a topology optimization based on the level set method using a superposition of Multiquadratic Radial Basis Functions (RBFs). Although topological changes that include the introduction of holes in the material domain are allowed, the method requires artificial parameters to represent the level set function, which greatly affect the obtained optimal configurations. Wei and Wang [64, 65] proposed a piecewise constant level set method used in their topology optimization method. In this method, an objective functional is formulated as the sum of a primary objective functional and a structural perimeter, which regularizes the optimization problem.

However, obtained optimal configurations can differ dramatically depending on the initial configuration, since the setting of certain parameters of the constraint functional for the piecewise constant level set function greatly affects the updating of the level set function.

1.4 Motivation and objective

This thesis presents a topology optimization method using a level set model incorporating a fictitious interface energy derived from the phase field concept, to overcome the numerical problems mentioned above. The presented method, a type of topology optimization method, also has the advantage of allowing not only shape but also topological changes. In addition, the presented method allows the geometrical complexity of the optimal configuration to be qualitatively specified, a feature resembling the perimeter control method, and does not require re-initialization operations during the optimization procedure.

1.5 Thesis organization

In the following chapters, a topology optimization problem is formulated based on the level set method, and the method of regularizing the optimization problem by introducing a fictitious interface energy is explained. The reaction-diffusion equation that updates the level set function is then derived. Here, we use the ersatz material approach to compute the equilibrium equations of the structure on an Eulerian coordinate system. Next, an optimization algorithm for the proposed method is constructed using the Finite Element Method. The proposed topology optimization method is then applied to the minimum mean compliance problem, the optimum design problem of compliant mechanisms, the lowest eigenfrequency problem the thermal problems. In addition, to confirm the validity and utility of the proposed topology optimization method, several numerical examples are provided for both two- and three-dimensional cases.

Chapter 2

Optimization method

2.1 Introduction

This chapter presents a new formulation of topology optimization method using level set-based structural boundary expressions and a fictitious interface energy, which is derived from concept of the phase field method. In the method, the level set function is updated using a reaction-diffusion equation, and not required re-initialization process [53, 78]. Note that in conventional methods [57, 59], the level set function is updated based on the Hamilton-Jacobi equation, since the structural optimization method is formulated based on the boundary advection concept.

This chapter is organized as follows: first, I briefly discuss the topology optimization problem and incorporating level set-based structural boundary expressions. Second, the topology optimization problem is regularized by incorporating a fictions interface energy. Next, a method updating the design variables is constructed. That is, the topology optimization problem is replaced by solving a reaction-diffusion equation.

2.2 Topology optimization problem

Consider a structural optimization problem that determines the optimal configuration of a domain filled with a solid material, i.e., a material domain Ω that denotes the design domain, by minimizing an objective functional F under a constraint functional G concerning the volume constraint, described as follows:

$$\inf_{\Omega} \quad F(\Omega) = \int_{\Omega} f(\mathbf{x}) \mathrm{d}\Omega \tag{2.1}$$

$$\text{subject to} \quad G(\Omega) = \int_{\Omega} \mathrm{d}\Omega - V_{\max} \leq 0, \tag{2.2}$$

where $V_{\max}$ is the upper limit of the volume constraint and $\mathbf{x}$ represents a point located in Ω. In conventional topology optimization methods [8], a fixed design domain D, composed of a material domain Ω such that $\Omega \subset D$, and another complementary domain representing a void exists, i.e., a void domain $D \setminus \Omega$ is introduced. Using the characteristic function $\chi_\Omega \in L^\infty$ defined as

$$\chi_\Omega(\mathbf{x}) = \begin{cases} 1 & \text{if} \quad \mathbf{x} \in \Omega \\ 0 & \text{if} \quad \mathbf{x} \in D \setminus \Omega, \end{cases} \tag{2.3}$$

the above structural optimization problem is replaced by a material distribution problem, to search for an optimal configuration of the design domain in the fixed design domain D as follows:

$$\inf_{\chi_\Omega} \quad F(\chi_\Omega(\mathbf{x})) = \int_D f(\mathbf{x}) \chi_\Omega(\mathbf{x}) \mathrm{d}\Omega \tag{2.4}$$

$$\text{subject to} \quad G(\chi_\Omega(\mathbf{x})) = \int_D \chi_\Omega(\mathbf{x}) \mathrm{d}\Omega - V_{\max} \leq 0. \tag{2.5}$$

In the above formulation, topological changes as well as shape change are allowed during the optimization procedure.

However, it is commonly accepted that topology optimization problems are ill-posed because the obtained configurations expressed by the characteristic function can be very discontinuous. That is, since the characteristic function χ is defined as a subset of a bounded Lebesgue space L^∞ which is only assured integrability, the obtained solutions may be discontinuous anywhere in the fixed design domain. To overcome this problem, the design domain is relaxed using various regularization techniques such as the homogenization method [22, 23, 24]. In the homogenization method, microstructures that represent the composite material status are introduced. In two-scale modeling, microstructures are continuously distributed almost everywhere in the fixed design domain D. The regularized and sufficiently continuous physical properties are obtained as the homogenized properties. Burger and Stainko [38], Wang and Zhou [33, 37] and Zhou and Wang [35, 34] proposed an alternative regularization method using the Tikhonov regularization method [79]. In these methods, by adding a Cahn-Hilliard-type penalization functional [29] to an objective functional, the topology optimization problem is regularized and the material density penalized. The phase field model utilized in certain structural optimization methods employs a regularization technique based on the imposition of some degree of shape smoothness, but these methods also yield optimal configurations that include grayscales.

In these regularization techniques, the existence of grayscales is allowed in the obtained optimal configurations. Although such grayscales can be interpreted as being micro-porous in the physical sense, they are problematic in the engineering sense since such obtained optimal solutions are difficult to interpret as practical designs that can be manufactured. Furthermore, the optimal configurations obtained by conventional topology optimization methods can include highly complex structures that are also inappropriate from an engineering and manufacturing standpoint. To mitigate these problems, a method using a perimeter constraint [42] and methods using a density gradient constraint [43, 44] have been proposed. In the former, however, the obtained results crucially depend on artificial parameters that require appropriate, but elusive, values to obtain desired results. And in the latter, use of the density gradient constraint increases grayscales. Also, methods employing perimeter or density gradient constraints are poor at adjusting the geometrical complexity of the obtained optimal configurations, since the relation of the geometrical complexity of the configuration and the optimization parameters cannot be uniquely determined. Hitherto, a method that allows the geometrical complexity of obtained optimal structures to be manipulated has not been proposed.

On the other hand, level set-based structural optimization methods have been proposed [45, 57, 59]. In these methods, the level set function $\phi(\mathbf{x})$ is introduced to represent a boundary $\partial\Omega$ between the material and void domains as shown in Figure 2.1. That is, the boundary is expressed using the level set function $\phi(\mathbf{x})$ as follows:

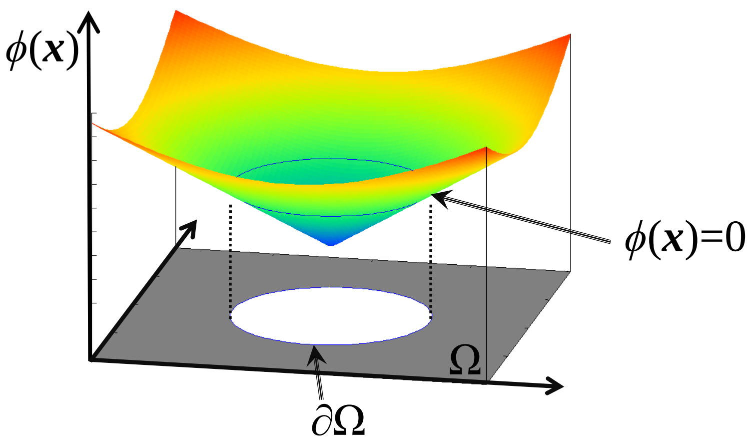

Figure 2.1: Level set function

$$\begin{cases} \phi(\mathbf{x}) > 0 & \text{for} \quad \forall \mathbf{x} \in \Omega \setminus \partial\Omega \\ \phi(\mathbf{x}) = 0 & \text{for} \quad \forall \mathbf{x} \in \partial\Omega \\ \phi(\mathbf{x}) < 0 & \text{for} \quad \forall \mathbf{x} \in D \setminus \Omega. \end{cases} \tag{2.6}$$

Using the above level set function, an arbitrary topology as well as shape of the material domain Ω in domain D can be implicitly represented, and level set boundary expressions are free of grayscales. In level set-based methods, the evolution of the boundaries with respect to fictitious times is tracked by solving the so-called Hamilton-Jacobi partial differential equation (explained below), with an appropriate normal velocity that is the velocity of the moving boundary normal to the interface. However, as Allarie *et al.* [59] discussed, this problem is basically ill-posed, and in order to regularize the structural optimization problems, certain smoothness, geometrical, or topological constraint, such as a perimeter constraint [42] must be imposed. Furthermore, topological changes that increase the number of holes in the material domain may not occur, although topological changes that decrease the number of holes are allowed. As a result, the obtained optimal configurations strongly depends on the given initial configuration.

2.3 Regularization technique

In this research, to overcome the above major problems in the conventional topology optimization methods and level set-based structural optimization methods, It is presented a new level set-based topology optimization method using a fictitious interface energy based on the phase field model.

In the proposed approach, first, the definition of the level set function is modified per the following equation to introduce the fictitious interface energy in the phase field model to regularize the topology optimization problem:

$$\begin{cases} 1 \geq \phi(\mathbf{x}) > 0 & \text{for} \quad \forall \mathbf{x} \in \Omega \setminus \partial\Omega \\ \phi(\mathbf{x}) = 0 & \text{for} \quad \forall \mathbf{x} \in \partial\Omega \\ 0 > \phi(\mathbf{x}) \geq -1 & \text{for} \quad \forall \mathbf{x} \in D \setminus \Omega. \end{cases} \tag{2.7}$$

It is assumed that the distribution of the level set function ϕ must have the same property of distribution as the phase field variable in the phase field method. Based on this assumption, the level set function ϕ has upper and lower limit constraints imposed in Equation (2.7). In addition, in sufficiently distant regions from the structural boundaries, the value of the level set function must be equivalent to 1 or -1.

Here, by adding a fictitious interface energy term derived from the concept of the phase field model to the objective functional, the regularized topology optimization problem is described using the relaxed characteristic function that is a function of the level set function, defined as follows:

$$\inf_{\phi} \quad F_R(\chi_\phi(\phi), \phi) = \int_D f(\mathbf{x})\chi_\phi(\phi)\mathrm{d}\Omega + \int_D \frac{1}{2}\tau \mid \nabla\phi \mid^2 \mathrm{d}\Omega \tag{2.8}$$

$$\text{subject to} \quad G(\chi_\phi(\phi)) = \int_D \chi_\phi(\phi)\mathrm{d}\Omega - V_{\max} \leq 0, \tag{2.9}$$

where F_R is a regularized objective functional and $\chi_\phi(\phi) \in L^2$ is a sufficiently smooth characteristic function, since the level set function ϕ is assumed to be continuous and is formulated as

$$\Phi = \{\phi(\mathbf{x}) | \phi(\mathbf{x}) \in H^1(D)\}. \tag{2.10}$$

As a result, the former optimization problem is replaced with a problem to minimize the energy functional, which is the sum of the objective functional and the fictitious interface energy, where $\tau > 0$ is a regularization parameter representing the ratio of the fictitious interface energy and the objective functional.

Note that the fictitious interface energy term here is equivalent to the so-called Chan-Hilliard energy, and it plays a very important role in regularizing the optimization problem. By introducing this term, the optimization problem is sufficiently relaxed and the obtained optimal configurations have sufficient smoothness. The optimization problem also becomes numerically stable. It is well-known that the Chan-Hilliard energy converges exactly to the perimeter. As a result, our optimal configurations are obtained under an implicitly imposed geometrical constraint. This regularization is called the Tikhonov regularization method, and details concerning its theoretical background are available in the literature [79, 80]. It is possible to control the degree of complexity of obtained optimal structures by adjusting the value of the regularization parameter τ. Strictly speaking, the regularization technique employed here is a perimeter constraint method, just as regularization techniques applied to the original topology optimization method implicitly impose geometric constraints. Note that Leitao and Scherzer [61] proposed a shape optimization method incorporating the Tikhonov regularization method and level set method, however the basic concept of their method differs from ours, which is a topology optimization method.

Next, the optimization problem represented by (2.8) and (2.9) is reformulated using Lagrange's method of undetermined multipliers. Let the Lagrangian be $\bar{F}$ and the Lagrange multiplier of the volume constraint be λ. The optimization problem is then formulated as

$$\begin{aligned}\inf_{\phi} \quad \bar{F}_R(\chi_\phi(\phi), \phi) &= \int_D f(\mathbf{x})\chi_\phi(\phi)\mathrm{d}\Omega \\ &\quad + \lambda\left(\int_D \chi_\phi(\phi)\mathrm{d}\Omega - V_{\max}\right) + \int_D \frac{1}{2}\tau \mid \nabla\phi \mid^2 \mathrm{d}\Omega \qquad (2.11) \\ &= \int_D \bar{f}(\mathbf{x})\chi_\phi(\phi)\mathrm{d}\Omega - \lambda V_{\max} + \int_D \frac{1}{2}\tau \mid \nabla\phi \mid^2 \mathrm{d}\Omega, \qquad (2.12)\end{aligned}$$

where the density function of the Lagrangian $\bar{f}(\mathbf{x})$ is such that $\bar{f}(\mathbf{x}) = f(\mathbf{x}) + \lambda$. The optimal configuration will be obtained by solving the above optimization problem.

Next, the necessary optimality conditions (KKT-conditions) for the above optimization problem are derived as follows:

$$\left\langle \frac{\mathrm{d}\bar{F}_R(\chi_\phi(\phi), \phi)}{\mathrm{d}\phi}, \Phi \right\rangle = 0, \quad \lambda G(\chi_\phi(\phi)) = 0, \quad \lambda \geq 0, \quad G(\chi_\phi(\phi)) \leq 0, \qquad (2.13)$$

where the notation $\left\langle \frac{\mathrm{d}\bar{F}_R(\chi_\phi(\phi),\phi)}{\mathrm{d}\phi}, \Phi \right\rangle$ represents the Fréchet derivative of the regularized Lagrangian $\bar{F}_R$ with respect to ϕ in the direction of Φ. The level set function describing the optimal configurations satisfies the above KKT conditions. Conversely, solutions obtained by Equation (2.13) are optimal solution candidates, but obtaining this level set function directly is problematic. Here, the optimization problem is replaced by a problem of solving time evolutional equations, which will provide optimal solution candidates.

2.4 The time evolutional equations

Let a fictitious time t be introduced, and assume that the level set function ϕ is also implicitly a function of t, to represent structural changes in the material domain Ω over time. In past level set-based structural optimization method research [57, 59], the outline of target structures is updated by solving the following time evolutional equation:

$$\frac{\partial \phi(\mathbf{x}, t)}{\partial t} + V_N(\mathbf{x}, t) \mid \nabla \phi(\mathbf{x}, t) \mid = 0 \qquad \text{in} \quad D \tag{2.14}$$

where $V_N(\mathbf{x}, t)$ is the normal velocity function, which is given as a smoothed shape derivative of material domain Ω since the above equation represents shape changes during fictitious optimization process times. Therefore, level set-based structural optimization methods using Equation (2.14) are essentially shape optimization methods. That is, only the shape boundary of the material domain evolves during the optimization process, and topological changes that generate holes in the material domain do not occur. As a result, the initial configuration settings profoundly affect the obtained optimal configuration.

To provide for the possibility of topological changes, Allaire *et al.* [70] proposed a method for introducing holes using topological derivatives, a concept that is basically the same as the bubble method [71] where the optimal position at which a hole is to be introduced is analytically derived. However, in Allaire's method, the obtained optimal structure depends on the setting of various parameters and it can be difficult to stably obtain optimal structures. Especially in problems where heat conduction and structural configuration are coupled, or static electric field, heat conduction and structural configuration are coupled, They encountered situations where convergence was poor and stably obtained optimal structures were elusive [69].

A new update method is developed in this research to replace the use Equation (2.14). Here, It is assumed that variation of the level set function $\phi(t)$ with respect to fictitious time t is proportional to the gradient of the Lagrangian $\bar{F}$, as shown in the following:

$$\frac{\partial \phi}{\partial t} = -K(\phi)\frac{\mathrm{d}\bar{F}_R}{\mathrm{d}\phi} \quad \text{in} \quad D, \tag{2.15}$$

where $K(\phi) > 0$ is a coefficient of proportionality. Substituting Equation (2.12) into Equation (2.15), I obtain the following:

$$\frac{\partial \phi}{\partial t} = -K(\phi)\Big(\frac{\mathrm{d}\bar{F}(\chi_\phi)}{\mathrm{d}\phi} - \tau\nabla^2\phi\Big) \quad \text{in} \quad D. \tag{2.16}$$

Here, note that the derivatives $\frac{\mathrm{d}\bar{F}(\chi_\phi)}{\mathrm{d}\phi}$ equivalent to the topological derivatives [72, 81, 82] defined as

$$D_T\bar{F} := \lim_{\epsilon \to 0} \frac{\bar{F}(\Omega_{\epsilon,\mathbf{x}}) - \bar{F}(\Omega)}{|\xi(\epsilon)|}, \tag{2.17}$$

where $\Omega_{\epsilon,\mathbf{x}} = \Omega - \bar{B}_\epsilon$ is the material domain with a hole, $\bar{B}_\epsilon$ is a sphere of radius ϵ centered at $\mathbf{x}$ and ξ is a function that decreases monotonically so that $\xi(\epsilon) \to 0$ as $\epsilon \to 0$, because the objective functional F is formulated using the characteristic function χ_ϕ. As a result, in our method, topological changes that increase the number of holes are allowed, since they are equivalent to the sensitivities with respect to generating structural boundaries in the material domain. In future work, I hope to discuss the theoretical connection between the characteristic function and topological derivatives in detail. On the other hand, the level set-based structural optimization method proposed by Wang *et al.* [57] is essentially a type of shape optimization method, since the sensitivities have non-zero values only on the structural boundaries.

Furthermore, It is assumed that the boundary condition of the level set function is a Dirichlet boundary condition on the non-design boundary, and a Neumann boundary condition on the other boundaries, to represent the level set function independently of the exterior of the fixed design domain D. Then, the obtained time evolutionary equation with boundary conditions are summarized as follows:

$$\begin{cases} \dfrac{\partial \phi}{\partial t} = -K(\phi)\Big(\dfrac{\mathrm{d}\bar{F}(\chi_\phi)}{\mathrm{d}\phi} - \tau\nabla^2\phi\Big) & \text{in } \; D \\ \dfrac{\partial \phi}{\partial n} = 0 & \text{on } \; \partial D \setminus \partial D_N \\ \phi = 1 & \text{on } \; \partial D_N. \end{cases} \tag{2.18}$$

Note that Equation (2.18) is a reaction-diffusion equation, and that the proposed method ensures the smoothness of the level set function.

Next, the time derivative of the regularized Lagrangian $\bar{F}_R$ is obtained using Equation (2.12) and (2.15) as follows:

$$\begin{aligned} \frac{d\bar{F}_R}{dt} &= \int_D \frac{\mathrm{d}\bar{F}_R}{\mathrm{d}\phi}\frac{\partial \phi}{\partial t} dD \\ &= \int_D \frac{\mathrm{d}\bar{F}_R}{\mathrm{d}\phi}\Big(-K(\phi)\frac{\mathrm{d}\bar{F}_R}{\mathrm{d}\phi}\Big) dD \quad \big(\because (2.15)\big) \\ &= -\int_D K(\phi)\Big(\frac{\mathrm{d}\bar{F}_R}{\mathrm{d}\phi}\Big)^2 dD \quad \leq 0. \end{aligned} \tag{2.19}$$

The above equation implies that when the level set function is updated based on Equations (2.16), the sum of the original Lagrangian $\bar{F}$ and the fictitious interface energy decreases monotonically.

2.5 Conclusions

This chapter presents a new formulation of topology optimization method using level set boundary expressions. The topology optimization problem is regularized using Tikhonov regularization method, that is, a fictions interface energy term is incorporated to the objective functional. Based on the formulation, KKT conditions is derived and the topology optimization is replaced by solving a reaction-diffusion equation.

Chapter 3

Numerical implementations

3.1 Introduction

In almost level set-based shape optimization methods, scheme of the Hamilton-Jacobi equation is discretized in the spatial direction using the Finite Difference Method [57, 59], since re-initialization techniques based on the Finite Element Method is very complicated. A design domain can be not discretized using nonstructural mesh, since the Finite Difference Method is used.

This chapter presents a numerical implementation method of above formulated topology optimization problem using Finite Element Method and a scheme of the system of the reaction-diffusion equation is presented. In addition, a finite element analysis method based on the level set-boundary expressions.

3.2 Optimization algorithms

The flowchart of the optimization procedure is shown in Fig. 3.1. As this figure shows, the initial configuration is first set. In the second step, the equilibrium equations are solved using the Finite Element Method. In the third step, the objective functional is computed. Here, the optimization process is finished if the objective

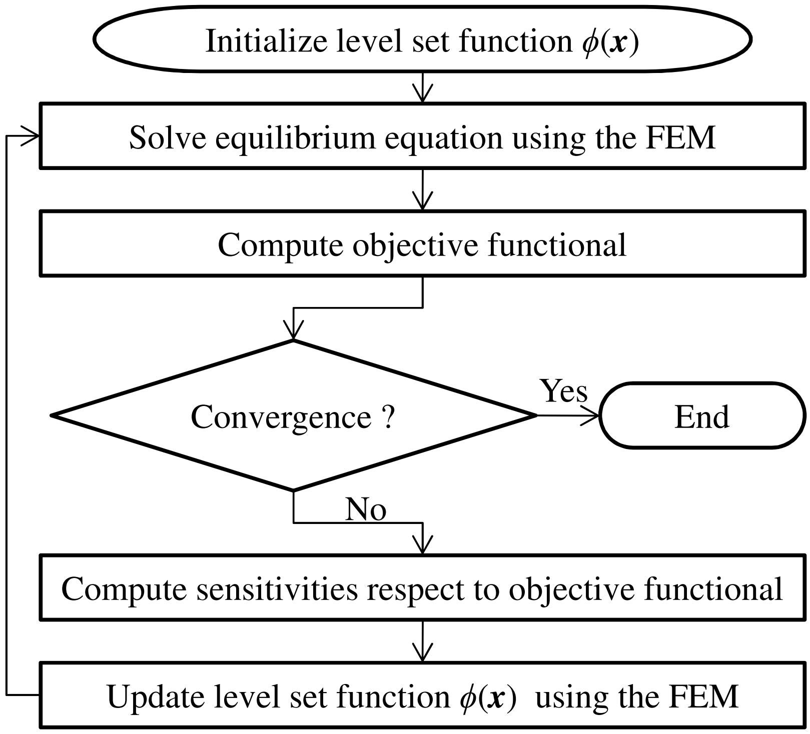

Figure 3.1: Flowchart of optimization procedure

functional has converged, otherwise the sensitivities with respect to the objective functional are computed. In the fourth step, the level set function ϕ is updated based on Eq.(2.18) using the Finite Element Method. Here, the Lagrange multiplier λ is estimated to satisfy the following:

$$G(\phi(t + \Delta t)) = 0. \tag{3.1}$$

In addition, the volume constraint is handled using the augmented Lagrangian method [83, 84, 85].

3.3 Scheme of the system of time evolutionary equations

This section presents develop a scheme for a system of time-evolutionary equations (2.18). First, I introduce a characteristic length L and an extended parameter C to normalize the sensitivities, and Equations (2.18) can then be replaced by dimensionless equations as follows.

$$\begin{cases} \dfrac{\partial \phi}{\partial t} = -K(\phi)\Big(C\frac{\mathrm{d}\bar{F}}{\mathrm{d}\phi} - \tau L^2 \nabla^2 \phi\Big) & \text{in} \quad D \\ \dfrac{\partial \phi}{\partial n} = 0 & \text{on} \quad \partial D \setminus \partial D_N \\ \phi = 1 & \text{on} \quad \partial D_N, \end{cases} \tag{3.2}$$

where C is defined as

$$C = \frac{c \int_D \mathrm{d}\Omega}{\int_D \mid \frac{\mathrm{d}\bar{F}}{\mathrm{d}\phi} \mid \mathrm{d}\Omega}. \tag{3.3}$$

Next, Equations (3.2) are discretized in the time direction using the Finite Difference Method as follows:

$$\begin{cases} \dfrac{\phi(t+\Delta t)}{\Delta t} - K(\phi(t))\tau L^2 \nabla^2 \phi(t+\Delta t) = -K(\phi(t))C\dfrac{\mathrm{d}\bar{F}}{\mathrm{d}\phi} + \dfrac{\phi(t)}{\Delta t} \\ \phi = 1 \qquad \text{on} \quad \partial D_N \\ \dfrac{\partial \phi}{\partial n} = 0 \qquad \text{on} \quad \partial D / \partial D_N, \end{cases} \tag{3.4}$$

where Δt is the time increment. Next, the above equations are translated to a weak form as follows, so they can be discretized using the Finite Element Method.

$$\begin{cases} \int_D \frac{\phi(t+\Delta t)}{\Delta t}\tilde{\phi} dD + \int_D \nabla^T \phi(t+\Delta t)\big(\tau L^2 K(\phi(t))\nabla\tilde{\phi}\big) dD \\ \qquad = \int_D \Big(-K(\phi(t))C\frac{\mathrm{d}\bar{F}}{\mathrm{d}\phi} + \frac{\phi(t)}{\Delta t}\Big)\tilde{\phi} dD \\ \qquad \text{for } \forall\tilde{\phi} \in \tilde{\Phi} \\ \phi = 1 \qquad \text{on} \quad \partial D_N, \end{cases} \tag{3.5}$$

where $\tilde{\Phi}$ is the functional space of the level set function defined by

$$\tilde{\Phi} = \{\phi(\mathbf{x}) | \phi(\mathbf{x}) \in H^1(D) \text{ with } \phi = 1 \text{ on } \partial D_N\}. \tag{3.6}$$

Discretizing Equation (3.5) using the Finite Element Method, the following equation is derived:

$$\begin{cases} \mathbf{T}\,\Phi(t+\Delta t) = \mathbf{Y} \\ \phi = 1 \qquad \text{on} \quad \partial D_N, \end{cases} \tag{3.7}$$

where $\Phi(t)$ is the nodal value vector of the level set function at time t and $\mathbf{T}$ and $\mathbf{Y}$ are described as follows:

$$\mathbf{T} = \bigcup_{j=i}^{e} \int_{V_e} \left(\frac{1}{\Delta t} \mathbf{N}^T \mathbf{N} + \nabla^T \mathbf{N} K(\phi(t)) \tau L^2 \nabla \mathbf{N} \right) dV_e \tag{3.8}$$

$$\mathbf{Y} = \bigcup_{j=i}^{e} \int_{V_e} \left(-K(\phi(t)) C \frac{\mathrm{d}\bar{F}}{\mathrm{d}\phi} + \frac{\phi(\mathbf{x}, t)}{\Delta t} \right) \mathbf{N} dV_e, \tag{3.9}$$

where e is the number of elements and $\bigcup_{j=i}^{e}$ represents the union set of the elements, j is the number of elements and $\mathbf{N}$ is the interpolation function of the level set function.

The upper and lower limit constraints of the level set function are not satisfied when the level set function is updated based on Eq. (3.7). To satisfy the constraints, the level set function is replaced based on the following rule after updating the level set function.

$$\text{if} \quad \|\phi\| > 1 \qquad \text{then} \quad \phi = \mathrm{sign}(\phi) \tag{3.10}$$

3.4 Approximated equilibrium equation

In this research the ersatz material approach is used [59]. That is, the equilibrium Equation (3.11) is approximated by Equation (3.12).

$$\int_D \boldsymbol{\epsilon}(\mathbf{u}) : \mathbf{E} : \boldsymbol{\epsilon}(\mathbf{v}) \chi \mathrm{d}\Omega = \int_{\Gamma_t} \mathbf{t} \cdot \mathbf{v} \mathrm{d}\Gamma + \int_D \mathbf{b} \cdot \mathbf{v} \chi \mathrm{d}\Omega \tag{3.11}$$

$$\int_D \boldsymbol{\epsilon}(\mathbf{u}) : \mathbf{E} : \boldsymbol{\epsilon}(\mathbf{v}) H_a(\phi) \mathrm{d}\Omega = \int_{\Gamma_t} \mathbf{t} \cdot \mathbf{v} \mathrm{d}\Gamma + \int_D \mathbf{b} \cdot \mathbf{v} H_a(\phi) \mathrm{d}\Omega, \tag{3.12}$$

where $H_a(\phi)$ is the Heaviside function approximated as

$$H_{a1}(\phi) = \begin{cases} d & (\phi < 0) \\ 1 & (0 \leq \phi) \end{cases} \tag{3.13}$$

or

$$H_{a2}(\phi) = \begin{cases} d & (\phi < -w) \\ \left(\frac{1}{2} + \frac{\phi}{w}\left(\frac{15}{16} - \frac{\phi^2}{w^2}\left(\frac{5}{8} - \frac{3}{16}\frac{\phi^2}{w^2}\right)\right)\right)(1-d) + d & (-w < \phi < w) \\ 1 & (w < \phi), \end{cases} \tag{3.14}$$

where w represents the width of transition and $d > 0$ represents the ratio of material constants, namely, the Young's modulus values between the void and material domains. Parameter d is introduced to ensure stable analyses of the fixed design domain when using the Finite Element method. In this research, the volume constraint function $G(\Omega)$ which is defined by Equation (2.9) is also approximated, as follows:

$$G(\phi) = \int_D H_g(\phi) \mathrm{d}\Omega - V_{\max}. \tag{3.15}$$

As shown in the following equation, $H_g(\phi)$ is the smoothed Heaviside function whose width of transition is 2, since as shown in Equation (2.7), the level set function values range from -1 to 1.

$$H_g(\phi) = \begin{cases} 0 & (\phi = -1) \\ \dfrac{1}{2} + \dfrac{\phi}{2}\left(\dfrac{15}{16} - \dfrac{\phi^2}{4}\left(\dfrac{5}{8} - \dfrac{3}{64}\phi^2\right)\right) & (-1 < \phi < 1) \\ 1 & (\phi = 1) \end{cases} \tag{3.16}$$

Note that intermediate regions between the material and void domains are not allowed in the approximation with respect to the material distribution (3.12), which eliminates grayscales completely. In the approximation with respect to the volume calculation (3.15), intermediate regions are allowed for numerical stability. Elimination of grayscales is important when using the equilibrium equations but is not important in the volume calculation.

3.5 Conclusions

This chapter presented a numerical implementation for presented level set-based topology optimization method. First of all, optimization algorithms is presented based on the flowchart. Next, numerical scheme the system of reaction-diffusion equations using the Finite Element Method is presented. In addition, scheme for solving an equilibrium equation based on the level set-boundary expressions is presented.

Chapter 4

The minimum mean compliance problem

4.1 Introduction

This cheaper presents an minimum mean compliance problem [8], which is most familiar application in shape and topology optimization field. First, the objective functional and the constraint functionals are formulated. Next, the sensitivities are derived using the adjoint variable method. Note that the adjoint problem is not necessary, since the minimum mean compliance problem is self adjoint problem. Finally, several numerical examples are show to confirm the validity and usefulness of presented method.

4.2 Formulation

Consider a material domain Ω where the displacement is fixed at boundary Γ_u and traction $\mathbf{t}$ is imposed at boundary Γ_t. A body force $\mathbf{b}$ may also be applied throughout the material domain Ω. Let the displacement field be denoted as $\mathbf{u}$ in the static equilibrium state. The minimum compliance problem is then formulated as follows:

$$\inf_{\phi} \ F_1(\chi) = l(\mathbf{u}) \tag{4.1}$$

$$\text{subject to} \ \ a(\mathbf{u},\mathbf{v}) = l(\mathbf{v}) \tag{4.2}$$

$$\text{for } \forall \mathbf{v} \in U \quad \mathbf{u} \in U$$

$$G(\chi) \leq 0 \tag{4.3}$$

where the notations in the above equation are defined as

$$a(\mathbf{u},\mathbf{v}) = \int_D \boldsymbol{\epsilon}(\mathbf{u}) : \mathbf{E} : \boldsymbol{\epsilon}(\mathbf{v}) \chi_\phi \mathrm{d}\Omega \tag{4.4}$$

$$l(\mathbf{v}) = \int_{\Gamma_t} \mathbf{t} \cdot \mathbf{v} \mathrm{d}\Gamma + \int_D \mathbf{b} \cdot \mathbf{v} \chi_\phi \mathrm{d}\Omega \tag{4.5}$$

$$G(\chi) = \int_D \chi \mathrm{d}\Omega - V_{\max}, \tag{4.6}$$

where $\boldsymbol{\epsilon}$ is the linearized strain tensor, $\mathbf{E}$ is the elasticity tensor, and

$$U = \{\mathbf{v} = v_i \mathbf{e}_i : \ v_i \in H^1(D) \text{ with } \mathbf{v} = 0 \text{ on } \Gamma_u\}. \tag{4.7}$$

Next, the sensitivity of Lagrangian $\bar{F}_1$ for the minimum mean compliance problem is derived. The Lagrangian $\bar{F}_1$ is the following:

$$\bar{F}_1 = l(\mathbf{u}) + a(\mathbf{u},\mathbf{v}) - l(\mathbf{v}) + \lambda G. \tag{4.8}$$

The sensitivity can be simply obtained using the adjoint variable method by

$$\left\langle \frac{\mathrm{d}\bar{F}_1}{\mathrm{d}\phi}, \Phi \right\rangle = \left\langle \frac{\partial l(\mathbf{u})}{\partial \mathbf{u}}, \delta\mathbf{u} \right\rangle \left\langle \frac{\partial \mathbf{u}}{\partial \phi}, \Phi \right\rangle + \left\langle \frac{\partial a(\mathbf{u},\mathbf{v})}{\partial \mathbf{u}}, \delta\mathbf{u} \right\rangle \left\langle \frac{\partial \mathbf{u}}{\partial \phi}, \Phi \right\rangle$$

$$+ \left\langle \frac{\partial a(\mathbf{u},\mathbf{v})}{\partial \phi}, \Phi \right\rangle + \lambda \left\langle \frac{\partial G}{\partial \phi}, \Phi \right\rangle \tag{4.9}$$

$$= \left\langle \frac{\partial \int_D (\boldsymbol{\epsilon}(\mathbf{u}) : \mathbf{E} : \boldsymbol{\epsilon}(\mathbf{v}) + \lambda)\chi_\phi \mathrm{d}\Omega}{\partial \phi}, \Phi \right\rangle, \tag{4.10}$$

where the adjoint field is defined as follows:

$$a(\mathbf{v},\mathbf{u}) = l(\mathbf{u}) \qquad \text{for } \forall \mathbf{u} \in U \quad \mathbf{v} \in U. \tag{4.11}$$

4.3 Numerical examples

4.3.1 Two-dimensional minimum mean compliance problems

In this subsection, several numerical examples are presented to confirm the utility and validity of proposed optimization method for two and three dimensional minimum compliance problems. In these examples, the isotropic linear elastic material has Young's modulus = 210 GPa, Poisson's ratio = 0.31 and parameter d in approximated Heaviside function (3.13) is set to 1×10^{-3}. Figure 4.1 shows the fixed design domain and the boundary conditions of model A and Figure 4.2 shows the same for model B.

Effect of the initial configurations

First, using model A, I examine the effect of different initial configurations upon the resulting optimal configurations. The regularization parameter τ is set to 1×10^{-4}, parameter c is set to 0.5 and the characteristic length L is set to 1m. Parameter $K(\phi)$

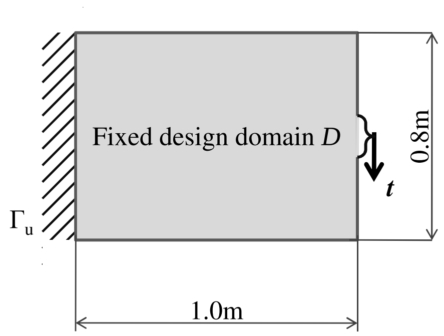

Figure 4.1: Fixed design domain and boundary conditions of model A

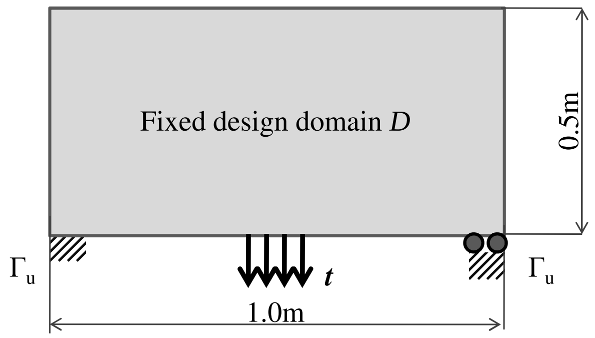

Figure 4.2: Fixed design domain and boundary conditions of model B

is set to 1, the upper limit of the volume constraint $V_{\max}$ is set to 40% of the volume of the fixed design domain and parameter d in approximated Heaviside function (3.13) is set to 1×10^{-3}.

The fixed design domain is discretized using a structural mesh and four-node quadrilateral plane stress elements whose length is 6.25×10^{-3}m. Figure 4.3 shows four cases and their obtained optimal configurations, each using a different initial configuration. The initial configuration for Case 1 has the material domain filled with material; for Case 2, the initial configuration has two holes; for Case 3, the initial configuration has many holes; and for Case 4, the initial configuration has material filling the material domain in the upper half of the fixed design domain. In all cases, the optimal configurations are smooth, clear and nearly the same. That is, an appropriate optimal configuration was obtained for all initial configurations. It is confirmed that the dependency of the obtained optimal configurations upon the initial configurations is extremely low.

Effect of finite element mesh size

Second, using model A, I examine the effect of the finite element mesh size upon the resulting optimal configurations. The regularization parameter τ is set to 8×10^{-5}, parameter c is set to 0.2, the characteristic length L is set to 1m, parameter $K(\phi)$ is set to 1, the upper limit of the volume constraint $V_{\max}$ is set to 40% of the volume of the fixed design domain and parameter d in approximated Heaviside function (3.13) is set to 1×10^{-3}. The initial configurations in all cases have the material domain filled with material in the Fixed design domain. The fixed design domain is discretized using a structural mesh and four-node quadrilateral plane stress elements. I examine three cases whose degree of discretization is subject to the following mesh parameters: 80×60, 160×120 and 320×240. Figure 4.4 shows the optimal configuration for each case. Again, all obtained optimal configurations are smooth, clear and practically

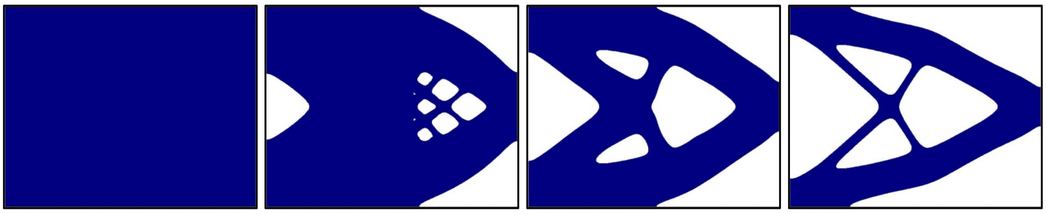

Initial configuration Step 10 Step 50 Optimal configuration

(a) Case 1

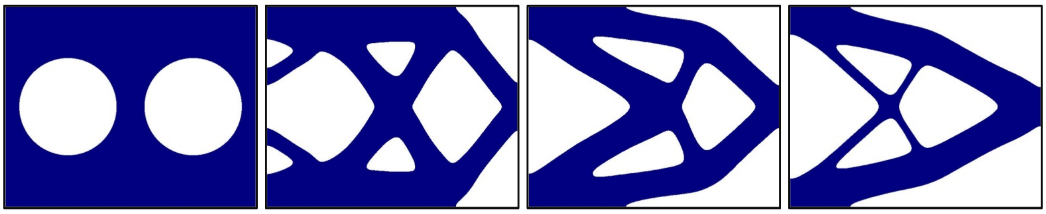

Initial configuration Step 10 Step 50 Optimal configuration

(b) Case 2

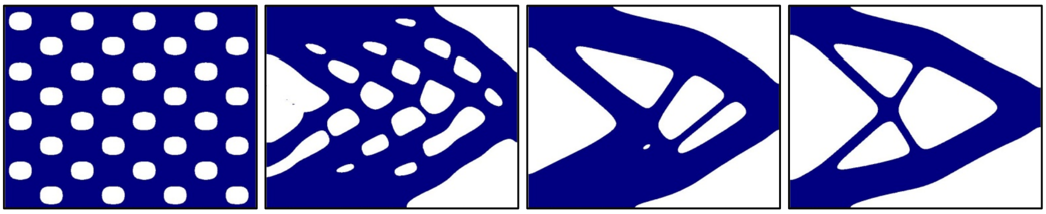

Initial configuration Step 10 Step 50 Optimal configuration

(c) Case 3

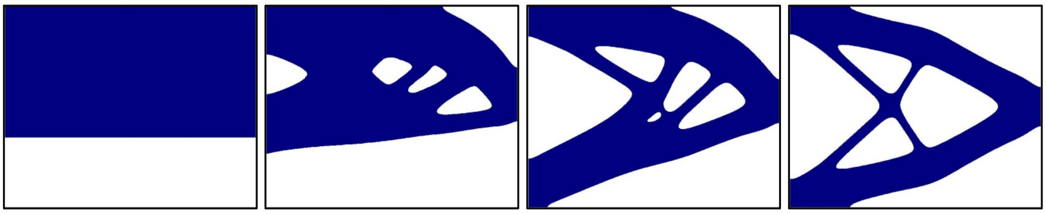

Initial configuration Step 10 Step 50 Optimal configuration

(d) Case 4

Figure 4.3: Initial configurations, intermediate results and optimal configurations

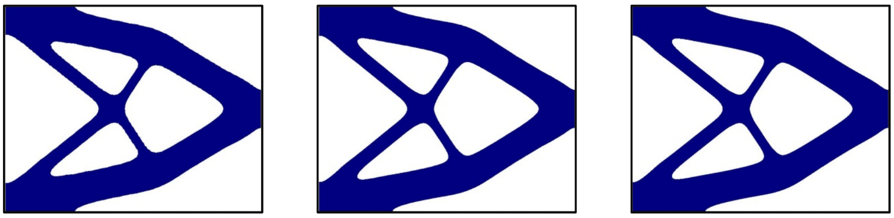

Figure 4.4: Optimal configurations: (a) 80×60 mesh; (b) 160×120 mesh; (c) 320×240 mesh

identical. That is, an appropriate optimal configuration can be obtained regardless of which degree of discretization was used here. It is confirmed that dependency with regard to the finite element mesh size is extremely small provided that the finite element size is sufficiently small.

Effect of the regularization parameter τ

I now examine the effect that different regularization parameter τ values have upon the resulting optimal configurations. In model A, parameter c is set to 0.5, the characteristic length L is set to 1m, parameter $K(\phi)$ is set to 1, the upper limit of the volume constraint $V_{\max}$ is set to 40% of the volume of the fixed design domain and parameter d in approximated Heaviside function (3.13) is set to 1×10^{-3}. The initial configuration in all case has the material domain filled with material in the fixed design domain. The fixed design domain is discretized using a structural mesh and four-node quadrilateral plane stress elements whose length is 6.25×10^{-3}m. I examine four cases where the regularization parameter τ is set to 5×10^{-4}, 5×10^{-5}, 3×10^{-5} and 2×10^{-5}, respectively. Figure 4.5 shows the optimal configuration for each case.

Next, using model B, parameter c is set to 0.5, the characteristic length L is set to 1m, and the upper limit of the volume constraint $V_{\max}$ is set to 50% of the volume of the fixed design domain. The initial configurations again have the material

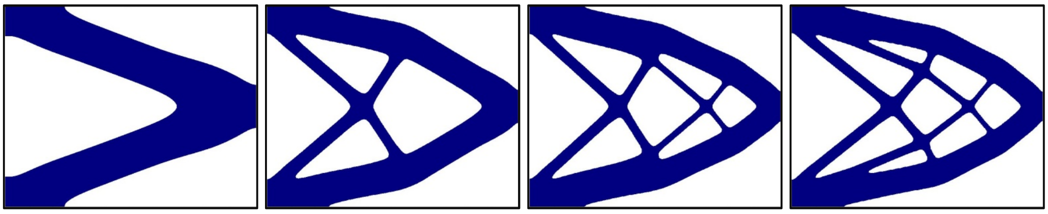

Figure 4.5: Optimal configurations: (a) $\tau = 5 \times 10^{-4}$; (b) $\tau = 5 \times 10^{-5}$; (c) $\tau = 3 \times 10^{-5}$; (d) $\tau = 2 \times 10^{-5}$

domain filled with material in the fixed design domain. The fixed design domain is discretized using a structural mesh and four-node quadrilateral plane stress elements whose length is 6.25×10^{-3}m. I examine four cases where the regularization parameter τ is set to 5×10^{-4}, 2×10^{-4}, 1×10^{-4} and 1×10^{-5}, respectively. Figure 4.6 shows the optimal configuration for each case. The obtained optimal configurations are smooth and clear and it can be confirmed that the use of the proposed method's τ parameter allows the complexity of the optimal structures to be adjusted at will.

Effect of the proportional coefficient $K(\phi)$

Next, I now examine the effect that different definitions of proportionality coefficient $K(\phi)$ have upon the resulting optimal configurations, using four initial configurations. The fixed design domain and boundary condition are shown in Figure 4.7. The isotropic linear elastic material has Young's modulus = 210 GPa, Poisson's ratio = 0.31 and parameter d and w in approximated Heaviside function (3.14) is set to 1×10^{-3} and 1, respectively. Parameter c is set to 0.5, the characteristic length L is set to 1m, regularization parameter τ is set to 5×10^{-4} and the upper limit of the volume constraint $V_{\max}$ is set to 40% of the volume of the fixed design domain. The fixed design domain is discretized using a structural mesh and four-node quadrilateral plane stress elements. I examine three cases, where the coefficient of proportionality

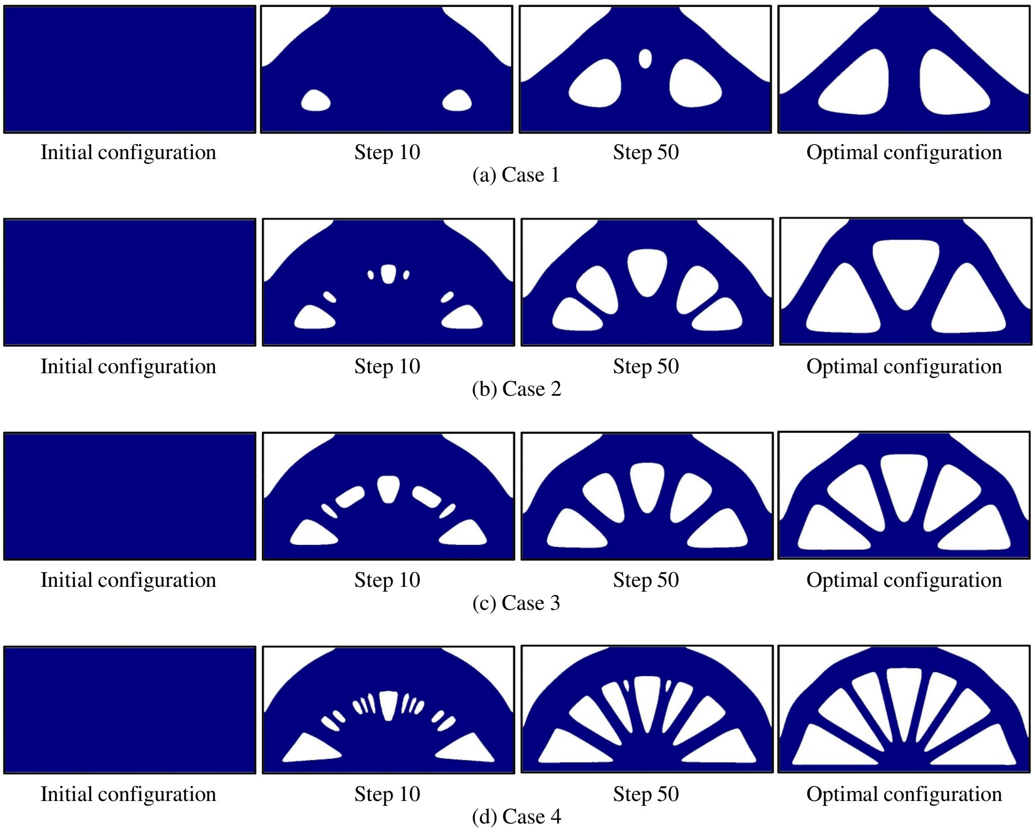

Figure 4.6: Initial configurations, intermediate results and optimal configurations: (a) $\tau = 5 \times 10^{-4}$; (b) $\tau = 2 \times 10^{-4}$; (c) $\tau = 1 \times 10^{-4}$; (d) $\tau = 1 \times 10^{-5}$

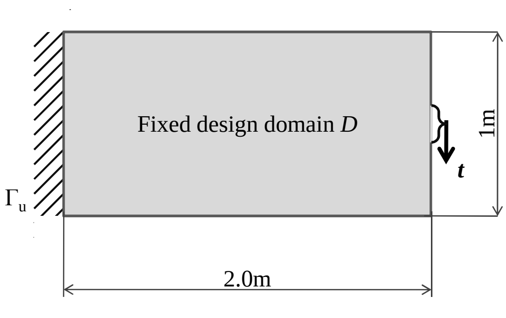

Figure 4.7: Fixed design domain and boundary conditions of model C

$K(\phi)$ is set as follows:

$$K_{\cos}(\phi) = \frac{1}{2} + \cos\left(\frac{\pi}{2}\phi\right) \tag{4.12}$$

$$K_{\sin}(\phi) = 1 + \frac{1}{2}\sin\left(\frac{\pi}{2}\phi\right) \tag{4.13}$$

$$K_1(\phi) = 1 \tag{4.14}$$

Figure 4.8 shows the different initial and optimal configurations for each case. In all

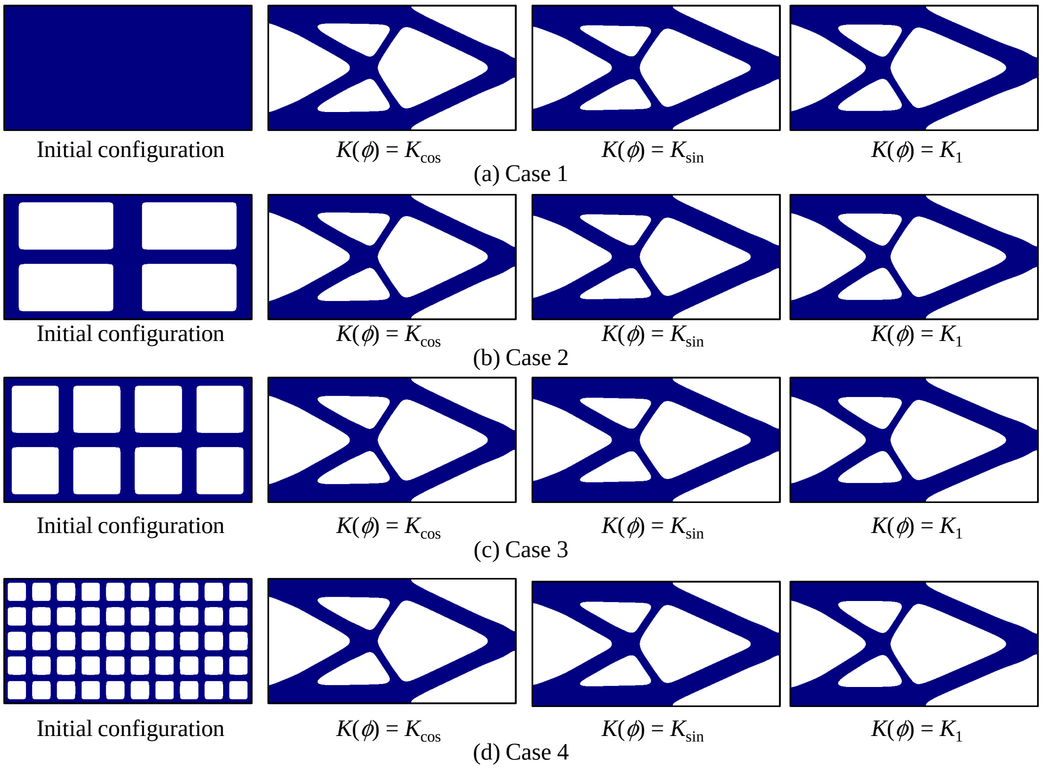

Figure 4.8: Initial configurations and optimal configurations

cases, the optimal configurations are smooth, clear and nearly the same. That is, an appropriate optimal configuration was obtained for all three definitions of $K(\phi)$, and it is confirmed that the dependency of the obtained optimal configurations upon these definitions is extremely low.

4.3.2 Three-dimensional minimum mean compliance problems

Effect of the regularization parameter τ

First, I now examine the effect that different values of the regularization parameter τ have upon the resulting optimal configurations in a three dimensional design problem. The isotropic linearly elastic material has Young's modulus = 210 GPa and Poisson's ratio = 0.31. Figure 4.9 shows the fixed design domain and boundary conditions. Parameter c is set to 0.5, the characteristic length L is set to 1m, and the upper limit

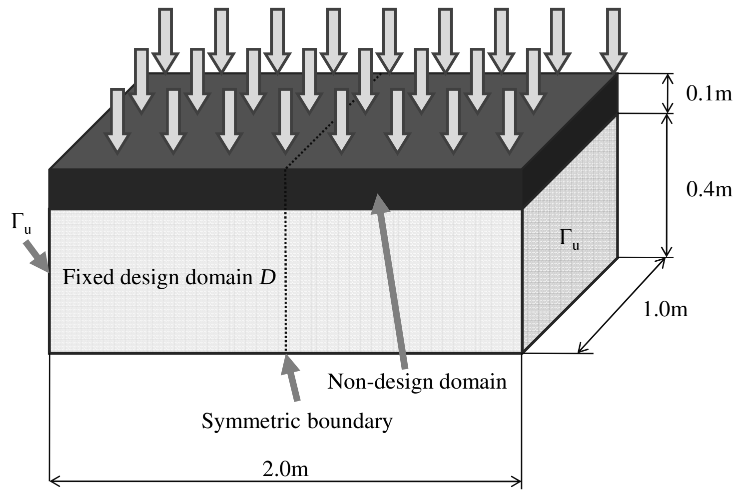

Figure 4.9: Fixed design domain and boundary conditions for three dimensional design problem

of the volume constraint $V_{\max}$ is set to 40% of the volume of the fixed design domain. The initial configurations have the material domain filled with material in the fixed design domain. The fixed design domain is discretized using a structural mesh and eight-node hexahedral elements whose length is 1×10^{-2}m. I examine two cases where the regularization parameter τ is set to 2×10^{-4} and 2×10^{-5}, respectively. Figure 4.10 shows the optimal configuration for each case. The obtained optimal configurations are smooth and clear, and I can be confirmed that the use of the proposed method's

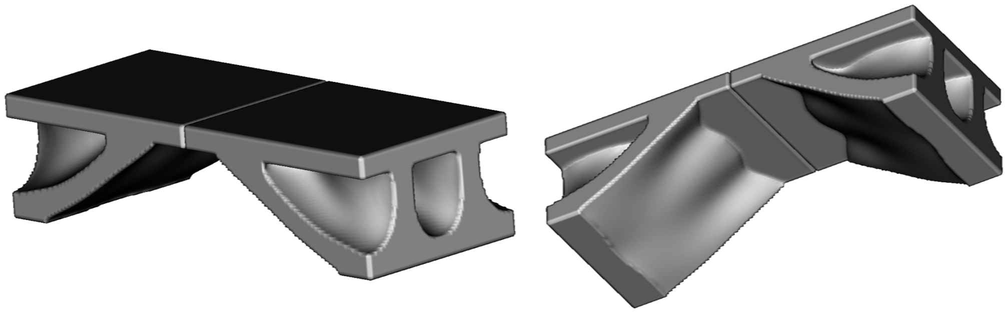

(a) Case 1

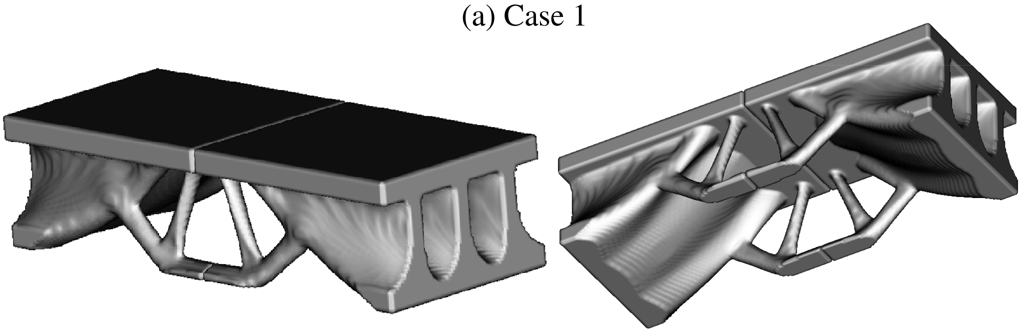

(b) Case 2

Figure 4.10: Optimal configurations: (a) $\tau = 2 \times 10^{-4}$; (b) $\tau = 2 \times 10^{-5}$

τ parameter allows the complexity of the optimal structures to be adjusted at will for the three-dimensional case as well.

Discretization using a nonstructural mesh

Second, I show a design problem of a mechanical part model where a nonstructural mesh is employed. The isotropic linear elastic material has Young's modulus = 210 GPa and Poisson's ratio = 0.31. The regularization parameter τ is set to 5×10^{-5}, parameter c is set to 0.5, the characteristic length L is set to 1m, and the upper limit of the volume constraint V_{max} is set to 45% of the volume of the design domain. The initial configurations have the material domain filled with material in the fixed design domain. Figure 4.11 shows the fixed design domain, boundary conditions and obtained optimal configuration. As shown, the obtained optimal configuration obtained by the proposed method is smooth and clear when a unstructublue mesh is

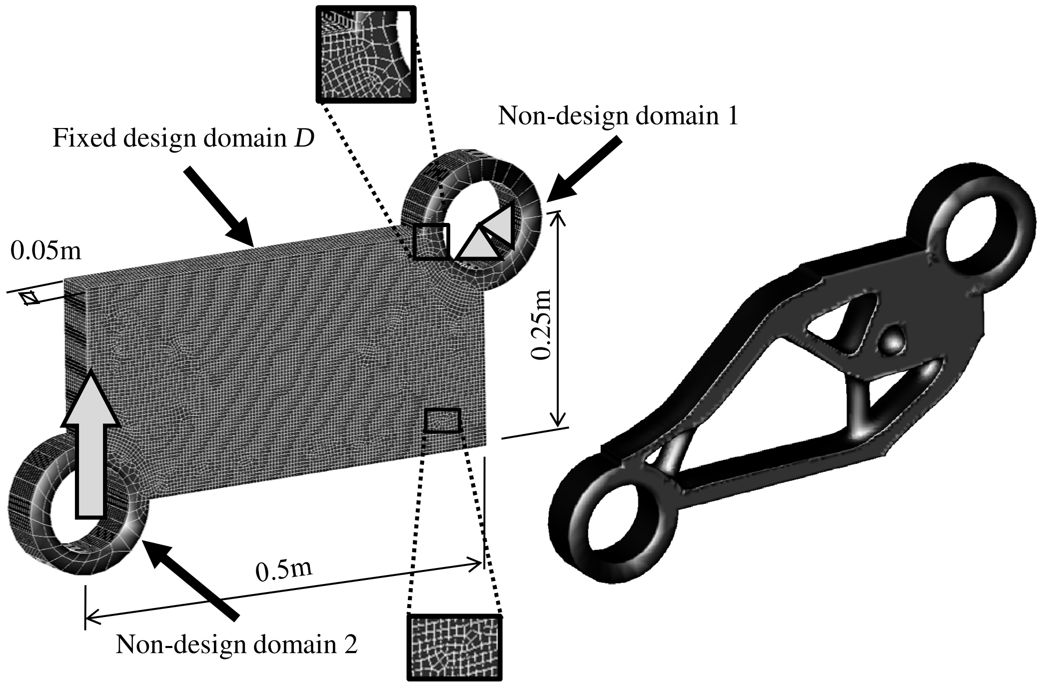

(a) Design domain and boundary conditions (b) Optimal configuration

Figure 4.11: Fixed design domain, boundary conditions and optimal configuration for a mechanical part model

used.

Uniform cross-section surface constraint

Next, I consider the use of a uniform cross-section surface constraint, which is important from a manufacturing standpoint. A geometrical constraint can easily be imposed by using an anisotropic variation of the regularization parameter τ. That is, if a component in the constraint direction of regularization parameter τ is set to a large value, the level set function will be constant in the constraint direction. As a result, in this scenario, obtained optimal configurations will reflect the imposition of a uniform cross-section surface constraint. Here, I show the effect that a uniform cross-section surface constraint has upon the obtained optimal configuration for a three-dimensional case. The isotropic linear elastic material has Young's modulus = 210 GPa and Poisson's ratio = 0.31. Figure 4.12 shows the fixed design domain and boundary conditions. Parameter c is set to 0.5, the characteristic length L is set to

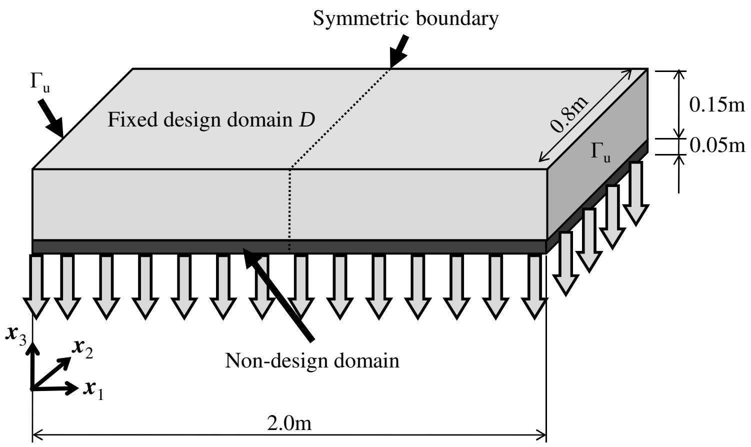

Figure 4.12: Fixed design domain and boundary conditions

1m, and the upper limit of the volume constraint $V_{\max}$ is set to 30% of the volume of the design domain. The initial configurations have the material domain filled with material in the fixed design domain. The fixed design domain is discretized using a structural mesh and eight-node hexahedral elements whose length is 1×10^{-2}m. Case (a) has an isotropic regularization parameter $\tau = 4 \times 10^{-5}$ as a non-uniform cross-section surface case. Case (b) has anisotropic component coefficients of the regularization parameter applied, where $\tau = 4 \times 10^{-5}$ in direction $\mathbf{x}_1$ and $\mathbf{x}_2$, and $\tau = 4$ in direction $\mathbf{x}_3$, so that a uniform cross-section constraint is imposed in direction $\mathbf{x}_3$. Figure 4.13 shows the optimal configuration for the two cases. The obtained optimal

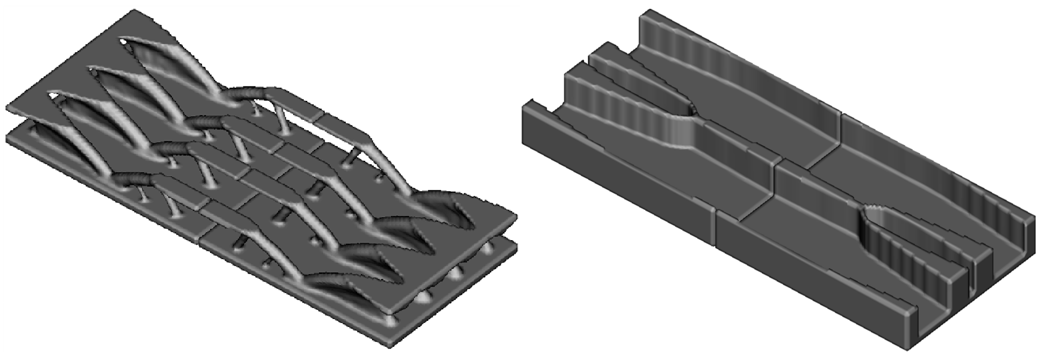

(a) Non-uniform cross-section surface (b) Uniform cross-section surface

Figure 4.13: Optimal configurations: (a) Non-uniform cross-section surface; (b) Uniform cross-section surface

configurations are smooth and clear, and it can be confirmed that our method can successfully impose a uniform cross-section surface constraint.

4.4 Conclusions

This chapter presents that a minimum mean compliance problem is applied to the presented level set-based topology optimization method and the several numerical examples are shown. It is confirmed that smooth and clear optimal configurations were obtained using the proposed topology optimization method, which also allows control of the geometrical complexity of the obtained optimal configurations. The obtained optimal configurations show minimal dependency upon the finite element size or initial configurations. In addition, it is showed that uniform cross-section surface constraints can easily be imposed by using an anisotropic variation of the regularization parameter τ

Chapter 5

The optimum design problem of compliant mechanisms

5.1 Introduction

Compliant mechanisms are a new type of mechanism that is intentionally designed to be flexible, to achieve a specified motion as a mechanism. Such mechanisms are widely applied in MEMS (Micro-Electro Mechanical Systems) since they are easily miniaturized and can be fabricated monolithically or from only a few parts [86, 87]. Moreover, compliant mechanisms can be used as thermal actuators by intentionally designing configurations that exploit thermal expansion effects in elastic materials when appropriate portions of the mechanism structure are heated or are subjected to an electric potential. Actuators of this type can provide comparatively large displacements and/or large forces at lower voltages, compared with electrostatic and piezoelectric actuators, and their advantages are increasingly exploited [87]. Such actuators are used in many micro-devices, such as monolithic silicon integrated optical micro-scanners [88], electrothermal vibromotors [89] and inchworm motors [90].

Several structural design methods for compliant actuators have been proposed.

Kwon *et al.* [90] and Setevenson *et al.* [91] developed design methods based on simple mechanics theory for the design of a thermoelastic linkage actuator and a bidirectional ring thermal actuator, respectively. Que *et al.* [92] obtained an optimal shape for a V-shaped electrothermal actuator based on sizing optimization using simple beam theory. Park *et al.* [93] designed rotary and linear actuators based on combinations of certain numbers of bent-beam electrothermal actuators. Chen *et al.* [94] performed sizing optimizations for an electrothermal microactuator using a Taguchi matrix. Wang *et al.* [95] designed cascade thermal actuator beams and performed parametric studies to investigate the best dimensional combinations. However, the methods used in the above research may not always provide high performance configurations, due to the relatively small number of design variables and parameter settings employed.

On the other hand, Sigmund [17] and Nishiwaki *et al.* [16] successfully applied topology optimization to the design of compliant mechanisms. However, topology optimization often suffers from numerical problems [40, 41] such as grayscales and hinges, and although several methods (e.g. [96, 97]) have been proposed to mitigate these problems, these depend on complex parameter settings. Several methods that attempt to minimize these problems have been proposed, such as the use of high-order finite elements [40], filtering schemes [41], and the perimeter control method [42]. Although certain filtering schemes, and the perimeter control method, are now popular means of avoiding these numerical problems, these methods crucially depend on artificial parameters for which there is no rational guideline for determining appropriate a priori parameter values.

To overcome above problems, this chapter present a new optimum design method of compliant mechanisms using presented topology optimization method. The outline of this chapter is as follows. First, an optimization problem is formulated that addresses the design of compliant mechanisms. Based on this formulation, the sensitivities are derived using adjoint variable method. Finally, several design examples are provided to confirm the usefulness of the presented topology optimization method.

5.2 Formulation

First, I clarify the design requirements of a compliant mechanisms, and formulate the objective function that can achieve the design requirements. Consider a material domain Ω for the compliant mechanisms where the displacement is fixed at boundary Γ_u. It is assumed that material domain Ω consists of an isotropic linearly elastic material.

In this chapter, I intend to design a compliant mechanisms that starts to deform in the direction of dummy vector $\mathbf{t}_{out}$ at boundary Γ_{out} in order to work as a mechanisms when traction $\mathbf{t}_{in}$ is applied at boundary Γ_{in}. To implement this function of the compliant mechanisms, the following two design specifications must be met: (a) sufficient flexibility to permit actuation, and (b) sufficient stiffness to maintain the structural shape when undergoing reaction traction caused by the presence of a workpiece.

Next, the objective function that can achieve the above design requirements is formulated using the mutual energy concept. Let us consider the two static equilibrium states. In both cases, the boundary Γ_u is fixed. Furthermore, in Case (1), a non-structural distributed spring representing the stiffness of the workpiece is located at boundary Γ_{out}, with a spring constant per unit length in the two-dimensional problem, or per unit area in three dimensions, of k, where the other boundary of the spring is fixed. In Case (2), traction $\mathbf{t}_{out}$ is imposed at boundary Γ_{out}. The displacement fields in Case (1) and Case (2) are described as $\mathbf{u}_1$ and $\mathbf{u}_2$, respectively.

Using the above two equilibriums, first, the objective function to achieve design requirement (a) is formulated. Here, It is introduced the mutual mean compliance formulated as,

$$l_2(\mathbf{u}_1) = \int_{\Gamma_{out}} \mathbf{t}_{out} \cdot \mathbf{u}_1 \mathrm{d}\Gamma. \tag{5.1}$$

This mutual mean compliance can be interpreted as a measure of the deformation $\mathbf{u}_1$ at boundary Γ_{out} when traction $\mathbf{t}_{in}$ is applied at boundary Γ_{in} and by maximizing $l_2(\mathbf{u}_1)$, sufficient flexibility concerning design requirement (a) is obtained. Note that for the design of the compliant mechanisms here, the goal is to maximize the displacement at the output port, and a specified deformation path is not required. Therefore, using the mean compliance for the objective functional is appropriate, because maximizing the mutual mean compliance is equivalent to maximizing the displacement in the direction given by fictitious traction vector $\mathbf{t}_{out}$.The mutual mean compliance derived from the energy norm is a physical criterion which is mathematically guaranteed to have a finite value during the optimization process, because solving the structural problem is equivalent to solving equilibrium equations expressed in a weak form, that is, to solving an energy balance equation.

Next, design requirement (b) is considered. In previous research work for the design of piezoelectric actuators based on the topology optimization method [98], the mean compliance computed according to the reaction force from the workpiece is simultaneously minimized as the mutual mean compliance is maximized, using a multi-objective optimization formulation. If this idea is applied to the design of a compliant mechanism, the mean compliance for a case having traction $-\mathbf{t}$, representing the reaction force from the workpiece at boundary Γ_{out}, is regarded as the objective function for design requirement (b), and both maximization of the mutual mean compliance and minimization of the mean compliance are simultaneously performed using the multi-objective function proposed in [16]. In this thesis, sufficient stiffness for archiving design requirement (b) is implicitly taken into account. That is, as a design setting, a non-structural distributed spring is located at boundary Γ_{out}, and sufficient stiffness at boundary Γ_{out} is obtained by maximizing the mutual mean compliance in Eq. (5.1), since this maximization provides a reaction force from the spring due to the deformation $\mathbf{u}_2$ at boundary Γ_{out}, and as a result, the stiffness is automatically maximized. Furthermore, the magnitude of the displacement and the stiffness at Γ_{out} can be simultaneously adjusted by changing the value of the spring constant, k. That is, by setting larger values for k, higher stiffness against the reaction force is obtained while the deformation $\mathbf{u}_2$ at boundary Γ_{out} is decreased. Conversely, by setting smaller spring constant values, a larger deformation $\mathbf{u}_2$ at boundary Γ_{out} is obtained while the stiffness against the reaction force is decreased.

Thus, the optimization problem is formulated, where a minus sign is prefixed to the objective function to transform the maximization problem to a minimization problem.

$$\inf_{\phi} \quad F_2(\chi) = l_2(\mathbf{u}_1) \tag{5.2}$$

$$\text{subject to} \quad a(\mathbf{u}_1, \mathbf{v}) = l_1(\mathbf{v}) \tag{5.3}$$

$$\text{for } \forall \mathbf{v} \in U \quad \mathbf{u} \in U$$

$$G(\chi) \leq 0, \tag{5.4}$$

where the notations in the above equation are defined as

$$l_1(\mathbf{v}) = \int_{\Gamma_{in}} \mathbf{t}_{in} \cdot \mathbf{v} \mathrm{d}\Gamma \tag{5.5}$$

$$l_2(\mathbf{v}) = \int_{\Gamma_{out}} \mathbf{t}_{out} \cdot \mathbf{v} \mathrm{d}\Gamma, \tag{5.6}$$

where $\mathbf{t}_{out}$ is a dummy traction vector representing the direction of the specified deformation at output port Γ_{out}. Based on Sigmund's formulation, a non-structural distributed spring is located at boundary Γ_{out}, and sufficient stiffness at boundary Γ_{out} is obtained by maximizing the mutual mean compliance, since this provides a reaction force from the spring due to the deformation at boundary Γ_{out}, which serves to automatically maximize the stiffness.

Next, the sensitivity of Lagrangian $\bar{F}_2$ for the design of compliant mechanisms is derived. The Lagrangian $\bar{F}_2$ is the following:

$$\bar{F}_2 = l_2(\mathbf{u}_1) + a(\mathbf{u}_1, \mathbf{v}) - l_1(\mathbf{v}) + \lambda G. \tag{5.7}$$

The sensitivity can be simply obtained using the adjoint variable method by

$$\begin{aligned} \left\langle \frac{\mathrm{d}\bar{F}_1}{\mathrm{d}\phi}, \Phi \right\rangle &= \left\langle \frac{\partial l_2(\mathbf{u}_1)}{\partial \mathbf{u}_1}, \delta \mathbf{u}_1 \right\rangle \left\langle \frac{\partial \mathbf{u}_1}{\partial \phi}, \Phi \right\rangle + \left\langle \frac{\partial a(\mathbf{u}_1, \mathbf{v})}{\partial \mathbf{u}_1}, \delta \mathbf{u}_1 \right\rangle \left\langle \frac{\partial \mathbf{u}_1}{\partial \phi}, \Phi \right\rangle \\ &\quad + \left\langle \frac{\partial a(\mathbf{u}_1, \mathbf{v})}{\partial \phi}, \Phi \right\rangle + \lambda \left\langle \frac{\partial G}{\partial \phi}, \Phi \right\rangle \qquad (5.8) \\ &= \left\langle \frac{\partial \int_D (\boldsymbol{\epsilon}(\mathbf{u}_1) : \mathbf{E} : \boldsymbol{\epsilon}(\mathbf{v}) + \lambda) \chi_\phi \mathrm{d}\Omega}{\partial \phi}, \Phi \right\rangle, \qquad (5.9) \end{aligned}$$

where the adjoint field is defined as follows:

$$a(\mathbf{v}, \mathbf{u}_1) = l_2(\mathbf{u}_1) \qquad \text{for } \forall \mathbf{u}_1 \in U \quad \mathbf{v} \in U. \tag{5.10}$$

5.3 Numerical examples

5.3.1 Two-dimensional compliant mechanism design problem

Next, our proposed method is applied to the problem of finding an optimum design for a compliant mechanism. The isotropic linear elastic material has Young's modulus = 210 GPa and Poisson's ratio = 0.31. Figure 5.1 shows the fixed design domain and boundary conditions. Parameter c is set to 0.5, characteristic length L is set to 100μm, regularization parameter τ is set to 1×10^{-4} and the upper limit of the volume constraint $V_{\max}$ is set to 25% of the volume of the fixed design domain. The approximated Heaviside function (3.14) is used. Parameter d is set to 1×10^{-3} and w is set to 1. The initial configurations have the material domain filled with material

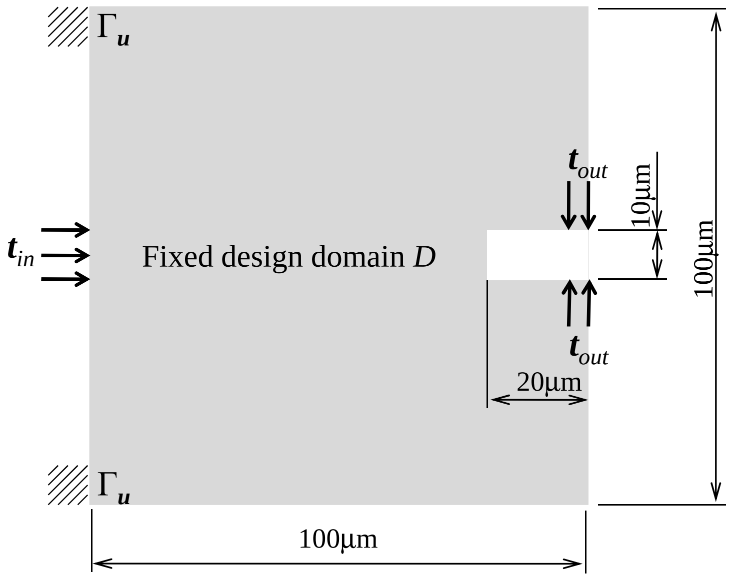

Figure 5.1: Fixed design domain for a two-dimensional compliant mechanism

in the fixed design domain. The fixed design domain is discretized using a structural mesh and four-node quadrilateral elements whose length is 0.5μm. Figure 5.2 shows the optimal configuration and the deformed shape. As shown, the obtained optimal configuration is smooth and clear, and it can be confirmed that the obtained optimal configuration deforms in the specified direction.

5.3.2 Three-dimensional compliant mechanism design problem

I applied the proposed method to a three-dimensional compliant mechanism design problem and consider the use of a uniform cross-section surface constraint. The isotropic linear elastic material has Young's modulus = 210 GPa and Poisson's ratio = 0.31. Figure 5.3 shows the fixed design domain and boundary conditions. Parameter c is set to 0.5, characteristic length L is set to 100μm and the upper limit of the volume constraint $V_{\max}$ is set to 20% of the volume of the fixed design domain. The

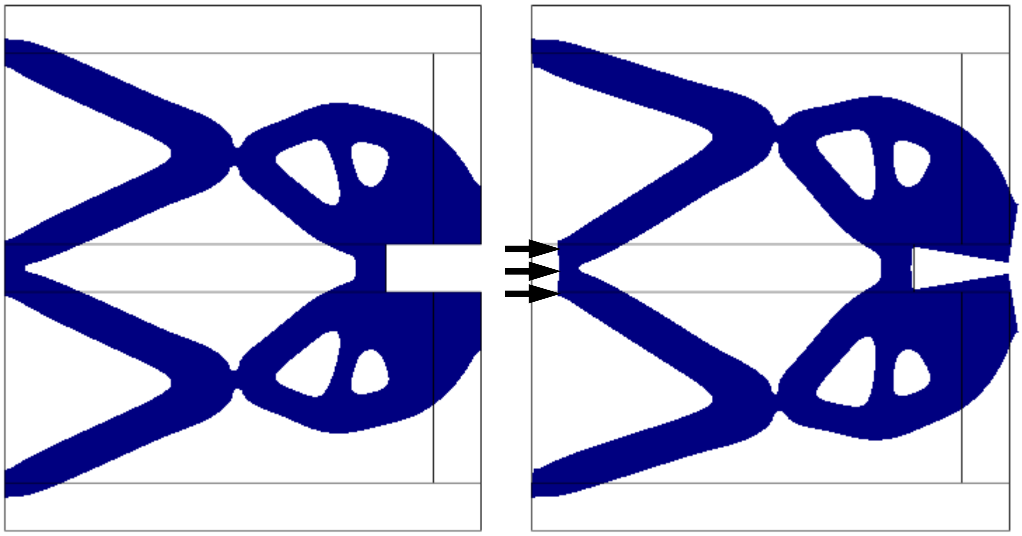

(a) Optimal configuration (b) Deformed shape

Figure 5.2: Configurations of the two-dimensional compliant mechanism (a) Optimal configuration; (b) Deformed shape

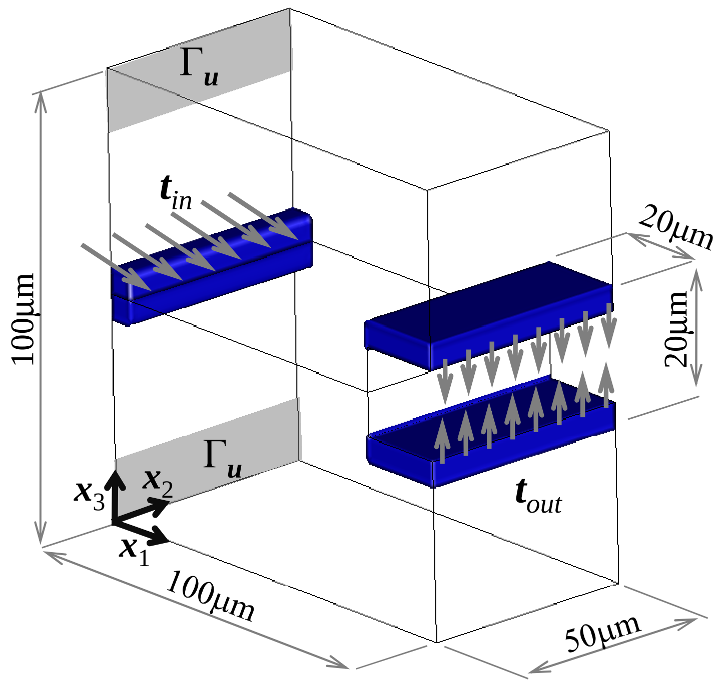

Figure 5.3: Fixed design domain for a three-dimensional compliant mechanism

approximated Heaviside function (3.14) is used, parameter d is set to 1×10^{-3} and w is set to 1. The initial configurations have the material domain filled with material in the fixed design domain. The fixed design domain is discretized using a structural mesh and eight-node hexahedral elements whose length is 1μm. Case (a) has an isotropic regularization parameter $\tau = 1 \times 10^{-4}$ as a non-uniform cross-section surface case. Case (b) has anisotropic component coefficients of the regularization parameter applied, where $\tau = 1 \times 10^{-4}$ in directions $\mathbf{x}_1$ and $\mathbf{x}_3$, and $\tau = 5 \times 10^{-1}$ in direction $\mathbf{x}_2$, so that a uniform cross-section constraint is imposed in direction $\mathbf{x}_2$. Figure 5.4 shows the optimal configurations. As shown, the obtained optimal configurations are smooth and clear, and it can be confirmed that our method can successfully impose a uniform cross-section surface constraint.

5.4 Conclusions

This chapter presented a topology optimization method for compliant mechanisms, based on the presented method. First of all, design requirements for the design of compliant mechanisms were clarified, the objective function was formulated based on the mutual energy concept and the optimization problem was formulated using this objective functional. Based on the formulation, the sensitivities are derived using adjoint variable method. Finally, two design problems were provided to examine the characteristics of the resulting optimal configurations. It was confirmed that the optimal configurations are free from hinge structures.

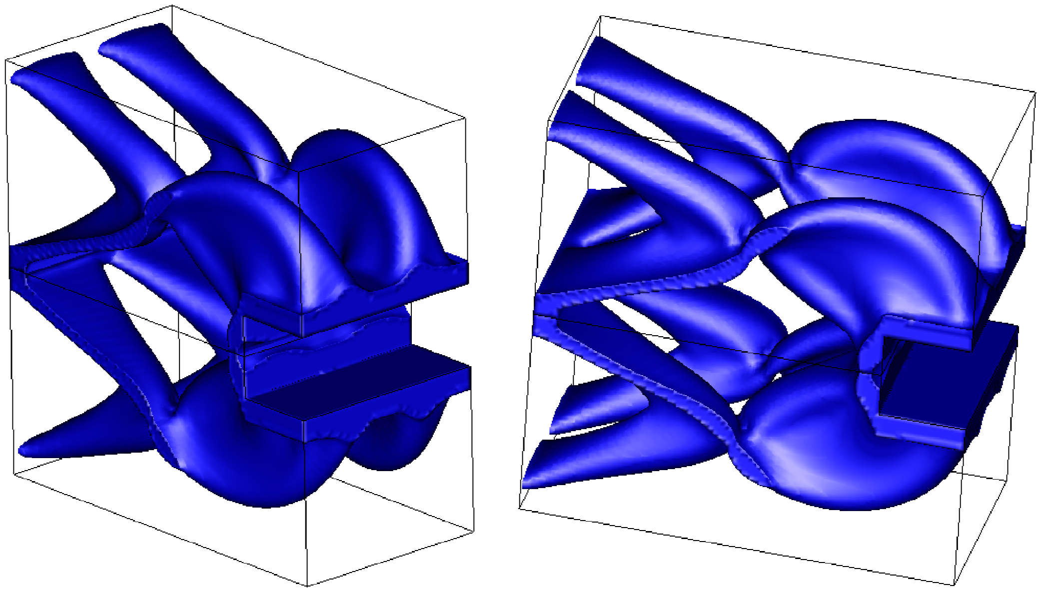

(a) Non-uniform cross-section surface

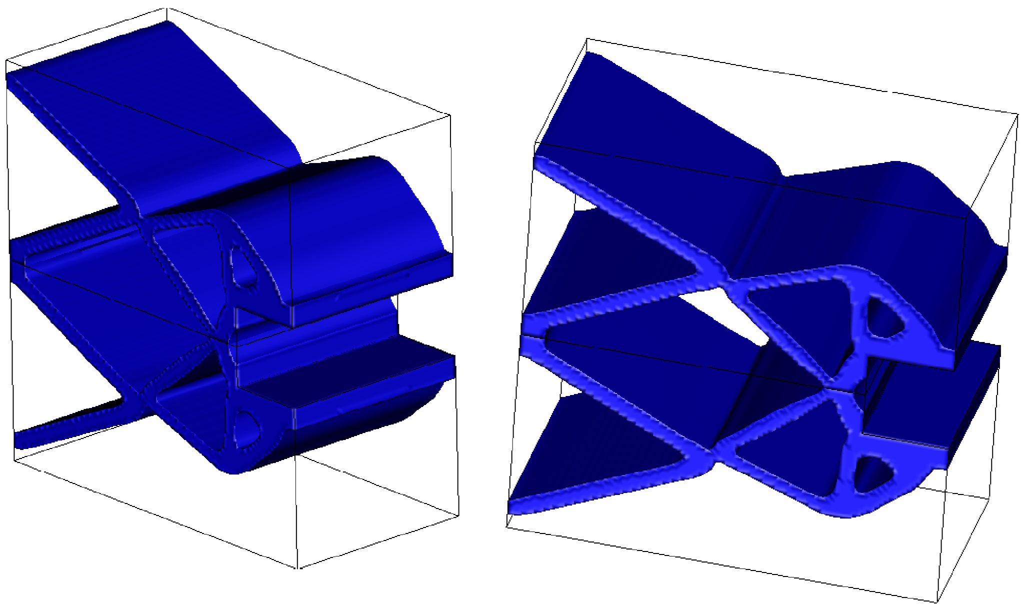

(b) Uniform cross-section surface

Figure 5.4: Configurations of the three-dimensional the compliant mechanisms: (a) Non-uniform cross-section surface (b) Uniform cross-section surface

Chapter 6

The lowest eigenfrequency maximization problem

6.1 Introduction

In mechanical structures, dynamic characteristics, especially vibration characters are crucial factors to determine the dynamic performance. For example, the lowest eigenfrequency is a measure for evaluation of dynamic stability. The higher dynamic performance can be obtained by maximizing the lowest eigenfrequency [13, 14].

On the other hand, a mechanical structure with high dynamic performance, such as mechanical resonators [99] and vibro motors [100], can be designed by utilizing resonance phenomena. The optimum design methods of such mechanical structures were proposed based on the conventional topology optimization methods.

This chapter present a new topology optimization method for the lowest eigenfrequency maximization problem based on the presented method. The outline of this chapter is follows. First, the objective functional formulated, and the sensitivities are derived based on the formulation and adjoint variable method. Two design examples are provided to confirm the presented topology optimization method.

6.2 Formulation

Consider a fixed design domain D with fixed boundary at Γ_u. The material domain Ω is filled with a linearly elastic material. The objective functional for the lowest eigenfrequency maximization problem can be formulated as follows:

$$\inf_{\phi} \quad F_3 = -\left(\sum_{k=1}^{q} \frac{1}{\omega_k^2}\right)^{-1} = -\left(\sum_{k=1}^{q} \frac{1}{\lambda_k}\right)^{-1}, \tag{6.1}$$

where ω_k is the k-th eigenfrequency, λ_k is k-th eigenvalue and q is an appropriate number of eigenfrequencies from the lowest eigen-mode. Therefore, the topology optimization problem, including the volume constraint, is formulated as follows:

$$\inf_{\phi} \quad F_3 = -\left(\sum_{k=1}^{q} \frac{1}{\lambda_k}\right)^{-1} \tag{6.2}$$

$$\text{subject to} \quad G \leq 0 \tag{6.3}$$

$$a(\mathbf{u}_k, \mathbf{v}) = \lambda_k b(\mathbf{u}_k, \mathbf{v}) \tag{6.4}$$

$$\text{for} \quad \forall \mathbf{v} \in U, \quad \mathbf{u}_k \in U, \quad k = 1, ..., q, \tag{6.5}$$

where the above notation $b(\mathbf{u}_k, \mathbf{v})$ is defined in the following equation,

$$b(\mathbf{u}_k, \mathbf{v}) = \int_{\Omega} \rho \mathbf{u}_k \cdot \mathbf{v} d\Omega, \tag{6.6}$$

where $\mathbf{u}_k$ is the corresponding k-th eigenmode and ρ is the density.

Next, the sensitivity of Lagrangian $\bar{F}_3$ for the design of compliant mechanisms is derived. The Lagrangian $\bar{F}_3$ is the following:

$$\bar{F}_3 = -\left(\sum_{k=1}^{q} \frac{1}{\lambda_k}\right)^{-1} + \sum_{k=1}^{q} \Big(a(\mathbf{u}_k, \mathbf{v}_k) - \lambda_k b(\mathbf{u}_k, \mathbf{v}_k) \Big) + \lambda G. \tag{6.7}$$

The sensitivity can be simply obtained using the adjoint variable method by

$$\left\langle \frac{\mathrm{d}\bar{F}_3}{\mathrm{d}\phi}, \Phi \right\rangle = \left(\sum_{k=1}^{q} \frac{1}{\lambda_k} \right)^{-2} \left[- \sum_{k=1}^{q} \frac{1}{\lambda_k^2} \left(\left\langle \frac{\partial a(\mathbf{u}_k, \mathbf{v})}{\partial \phi}, \Phi \right\rangle - \lambda_k \left\langle \frac{\partial b(\mathbf{u}_k, \mathbf{v})}{\partial \phi}, \Phi \right\rangle \right) \right] + \lambda \left\langle \frac{\partial G}{\partial \phi}, \Phi \right\rangle, \tag{6.8}$$

where the adjoint field is defined as follows:

$$a(\mathbf{u}_k, \mathbf{v}) = \lambda_k b(\mathbf{u}_k, \mathbf{v}) \qquad \text{for } \forall \mathbf{u} \in U \quad \mathbf{v} \in U. \tag{6.9}$$

6.3 Numerical example

6.3.1 Two-dimensional design problem

Finally, the proposed method is applied to the lowest eigenfrequency maximization problem. The isotropic linear elastic material has Young's modulus = 210 GPa, Poisson's ratio = 0.31 and mass density = $7,850\text{kg/m}^3$. Figure 6.1 shows the fixed design domain and boundary conditions for the two-dimensional lowest eigenfrequency maximization problem.

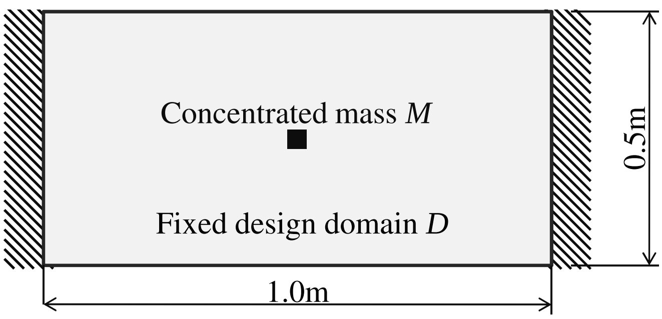

Figure 6.1: Fixed design domain for the two-dimensional the lowest eigenfrequency maximization problem

As shown, the right and left sides of the fixed design domain are fixed and a concentrated mass M = 1kg is set at the center of the fixed design domain. The fixed design domain is discretized using a structural mesh and four-node quadrilateral elements whose length is 5×10^{-3}m. Parameter c is set to 0.5, characteristic length L is set to 1m, $K(\phi)$ is set to 1 and the upper limit of the volume constraint $V_{\max}$ is set to 50% of the volume of the fixed design domain. The Approximated Heaviside function (3.13) is used, and parameter d is set to 1×10^{-2}. I examine three cases where parameter τ is set to 1.0×10^{-4}, 1.0×10^{-5}, and 1.0×10^{-6}, respectively. Figure 6.2 shows the obtained optimal configurations. The obtained optimal configurations

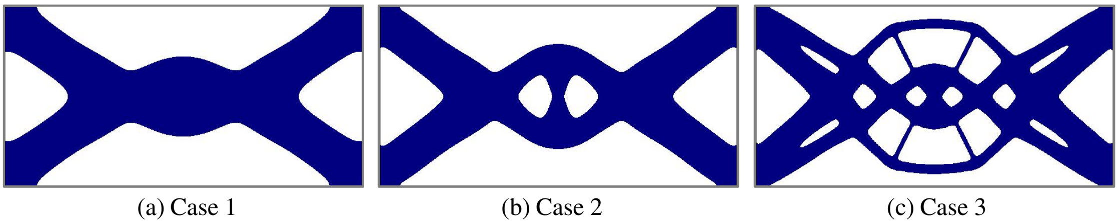

Figure 6.2: Optimal configurations for the two-dimensional lowest eigenfrequency maximization problem: (a) regularization parameter $\tau = 1.0\times10^{-4}$; (b) regularization parameter $\tau = 1.0 \times 10^{-5}$; (c) regularization parameter $\tau = 1.0 \times 10^{-6}$

are smooth and clear, and it can be confirmed that the use of the proposed method's τ parameter allows the complexity of the optimal structures to be adjusted at will for the lowest eigenfrequency maximization problem as well.

6.3.2 Three-dimensional design problem

Figure 6.3 shows the fixed design domain and boundary conditions for a three-dimensional lowest eigenfrequency maximization problem. The isotropic linear elastic material has Young's modulus = 210 GPa, Poisson's ratio = 0.31, mass density = $7,850\text{kg/m}^3$ and a concentrated mass M = 80kg is set at the center of the fixed design domain. The fixed design domain is discretized using a structural mesh and

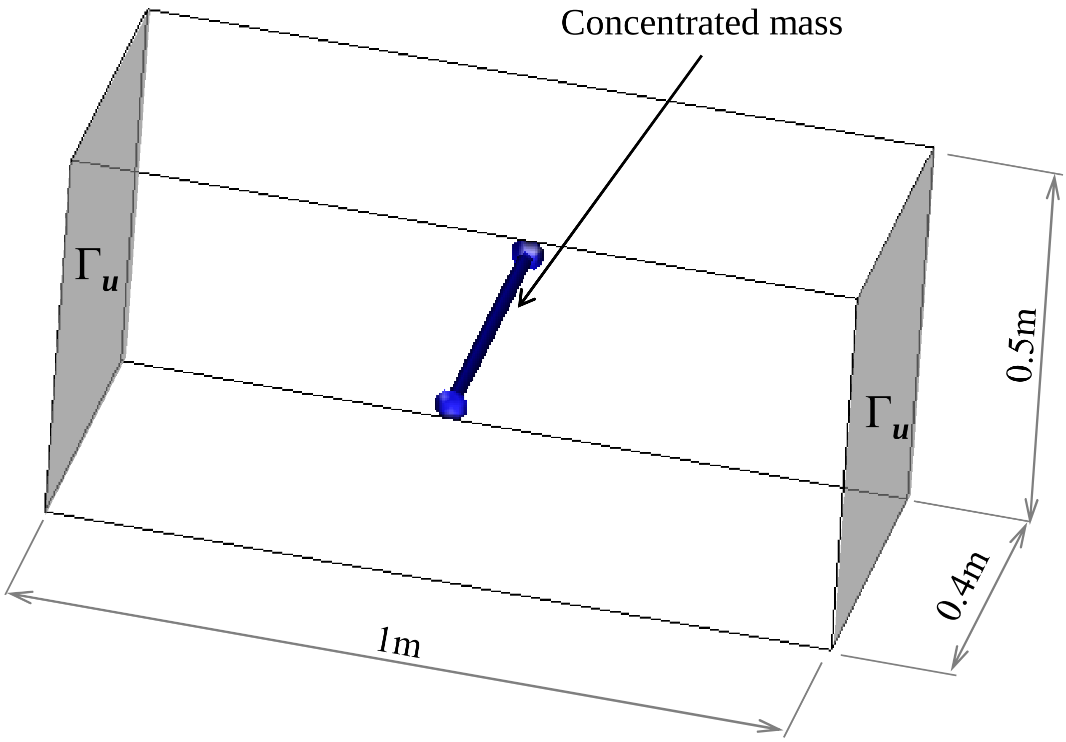

Figure 6.3: Fixed design domain for the three-dimensional lowest eigenfrequency maximization problem

eight-node hexahedral elements whose length is 1×10^{-3}m. Parameter c is set to 0.5, characteristic length L is set to 1m, $K(\phi)$ is set to 1 and the upper limit of the volume constraint $V_{\max}$ is set to 30% of the volume of the fixed design domain. The Approximated Heaviside function (3.13) is used, and parameter d is set to 1×10^{-2}. Figure 6.4 shows the optimal configurations. As shown, the obtained optimal configurations

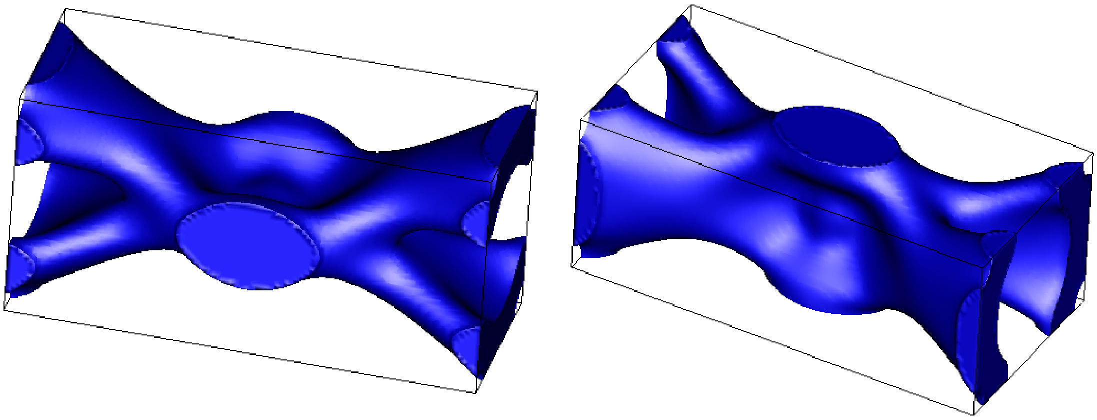

Figure 6.4: Optimal configurations of the three-dimensional lowest eigenfrequency maximization problem

are smooth and clear.

6.4 Conclusion

This chapter presented the lowest eigenfrequency maximization problem based on the presented level set-based topology optimization method. First of all, the objective functional was formulated, and the sensitivities were derived using adjoint variable method. Finally, two- and three-dimensional design problems were provided to examine the characteristics of the resulting optimal configurations. It was confirmed that obtained optimal configurations are clear and smooth and the geometrical complexity can be qualitatively specified by changing a regularization parameter τ.

Chapter 7

Thermal problems

7.1 Introduction

This chapter discusses a level set-based topology optimization method for maximizing thermal diffusivity in problems that deal with generic heat convection boundaries and include design-dependent boundary conditions.

For structural designs of heat engines such as diesel engines and steam turbines, maximization of thermal diffusivity in certain portions of the structure is an important factor that can enable reduction in operating temperatures and increased product durability. One way to obtain design solutions incorporating maximizations of thermal diffusivity and stiffness is to apply a topology optimization method.

However, when conventional topology optimization methods are used, the obtained optimal configurations may include grayscales since the optimal configurations are represented as density distributions in the fixed design domain. Moreover, highly complex configurations such as checkerboard patterns may exist in the optimal solutions, and such complex configurations are problematic in an engineering sense. Furthermore, in conventional topology optimization methods using these regularization techniques, structural boundaries cannot be explicitly defined. Therefore, optimization problems that incorporate design-dependent boundary conditions, such as heat convection boundary conditions and pressure load problems, cannot be easily handled, since the boundary conditions must be assigned along structural boundaries in such design problems. Although Gao *et al.* [101] proposed a topology optimization method for heat conduction problems including design dependent effects using ESO (Evolutionary Structural Optimization), heat convection effects were not considered. Iga *et al.* [20] proposed a topology optimization method for maximizing thermal diffusivity using a homogenization design method, and included design-dependent boundary conditions, however in this method, shape dependencies with respect to heat transfer coefficients were considered based on an ad hoc procedure, where it was assumed that the shape dependencies could be replaced by the average value of the near-density value, and that the heat transfer coefficients were a function of this average value. Yoon and Kim proposed a topology optimization method for thermal problems considering design-dependent boundary conditions with respect to heat transfer boundaries, using the Element Connectivity Parameterization (ECP) [102] method, however theoretical discussions with respect to continuum mechanics were not provided. For pressure load problems, Chen and Kikuchi [103] proposed a structural topology optimization method considering pressure loads, where such loads were implicitly imposed on the structural boundaries via fictitious fluid elements in the void domain, without setting pressure loads on structural boundaries directly, so that design-dependent effects concerning pressure loads could be treated during the optimization procedure.

This chapter presents a level set-based topology optimization method for generic thermal problems that takes into account design-dependent boundary conditions due to heat convection, based on the level set method and the concept of the phase field theory. First, an optimization problem is formulated for generic thermal problems, using the concept of total potential energy. Based on the formulations, the sensitivities are derived using adjoint variable method. Finally, several numerical examples are provided to confirm the utility of the proposed topology optimization method.

7.2 Formulation

First of all, a steady-state thermal problem is considered. Suppose that an an arbitrary linear thermal conductor occupies domain Ω in the fixed design domain D. The temperature $u_t = T_0$ is prescribed at boundary Γ_t, a heat flux q is imposed at boundary Γ_q and a heat convection load consisting of heat convection coefficient h and ambient temperature $u_t = T_{amb}$ is imposed at structural boundary Γ_h. As shown in the following equations, the thermal problem of maximizing the temperature diffusivity of the structure is formulated as a problem to maximize the total potential energy $\Pi(u_t)$ [20]. Note that in the formulation of the objective functional below, a minus sign is added to reformulate the maximization problem as a minimization problem.

$$\inf_{\phi} \quad F_4 = -\Pi(u_t) = -\left(\frac{1}{2}a(u_t, u_t) - l(u_t)\right) \tag{7.1}$$

$$\text{subject to} \quad a(u_t, v_t) = l(v_t) \tag{7.2}$$

$$\text{for } \forall v_t \in U \quad u_t \in U_t$$

$$G(\Omega(\phi)) \leq 0 \tag{7.3}$$

where items in the above equations are defined as follows:

$$a(u_t, v_t) = \int_D \nabla u_t \boldsymbol{\kappa} \nabla v_t \chi_\Omega \mathrm{d}\Omega - \int_{\Gamma_h(\phi)} h u_t v_t \mathrm{d}\Gamma \tag{7.4}$$

$$l(v_t) = \int_{\Gamma_q} q v_t \mathrm{d}\Gamma + \int_D Q v_t \mathrm{d}\Omega - \int_{\Gamma_h(\phi)} T_{amb} v_t \mathrm{d}\Gamma \tag{7.5}$$

$$G(\Omega(\phi)) = \int_D \chi_\Omega \mathrm{d}\Omega - V_{\max} \tag{7.6}$$

In addition, $\boldsymbol{\kappa}$ is the thermal conduction tensor, $V_{\max}$ is the upper limit of the volume constraint and U_t is a subset of a Sobolev space in which admissible temperatures are defined as

$$U_t = \{v_t \in H^1(D) \text{ with } v_t = T_0 \text{ on } \Gamma_t\} \tag{7.7}$$

Next, KKT-conditions for the above optimization problem, and the sensitivities, are derived. Let $\bar{F}$ be a Lagrangian formulated as

$$\begin{aligned} \bar{F}_4 = &-\frac{1}{2}a(u_t, u_t) + l(u_t) \\ &+ a(u_t, v_t) - l(v_t) + \lambda G(\Omega(\phi)) \end{aligned} \tag{7.8}$$

where λ is the Lagrange multiplier and v_t is the adjoint temperature field. The KKT-conditions are then derived as

$$\begin{aligned} &\frac{\mathrm{d}\bar{F}_4}{\mathrm{d}\phi} = 0, \quad a(u_t, v_t) - l(v_t) = 0, \\ &\lambda G = 0, \quad \lambda \geq 0, \quad G \leq 0 \end{aligned} \tag{7.9}$$

Here, the adjoint equation is defined as

$$a(v_t, u_t) = l(u_t) \qquad \text{for } \forall u_t \in U_t \quad v_t \in U_t \tag{7.10}$$

Using equilibrium Equation (7.2) and substituting Equation (7.8) into Equation (7.10), I have

$$\bar{F}_4 = \frac{1}{2}a(u_t, v_t) + \lambda G(\Omega(\phi)) \tag{7.11}$$

Therefore, the derivative of $\bar{F}_4$ is given by

$$\left\langle \frac{\mathrm{d}\bar{F}_4}{\mathrm{d}\phi}, \Phi \right\rangle = \frac{1}{2}\left\langle \frac{\partial a(u_t, v_t)}{\partial \phi}, \Phi \right\rangle + \lambda \left\langle \frac{\partial G}{\partial \phi}, \Phi \right\rangle, \tag{7.12}$$

.

7.3 Numerical examples

Several example problems concerning heat conduction, internal heat generation and heat convection are now presented to confirm the utility of the proposed level set-based topology optimization method. The thermal conductivity is set to 148W/m · K for all of the following examples.

7.3.1 Heat conduction problem

I first consider a heat conduction problem, and Figure 7.1 shows the fixed design domain and boundary conditions. As shown, the fixed design domain has a prescribed temperature of 25°C at the center of the bottom line and a heat flux $q = 1.0$W/m is provided at left and right segments of the top line. The fixed design domain is discretized into four-node elements 1×10^{-4}m in length. The upper limit of the volume constraint $V_{\max}$ is set to 30% of the fixed design domain and parameter K is set to 1. The regularization parameter τ is set to 5×10^{-3}, parameter c is set to 0.5 and the characteristic length L is set to 1×10^{-2}m. Here, I examine the effect that different initial configurations have upon the resulting optimal configurations, as shown in Figure 7.2. Case 1 is an initial configuration with no holes, Case 2 has four holes initially, and Case 3 has many holes to begin with. Figure 7.2 shows the initial, intermediate and optimal configurations for these three cases. It can be confirmed that proposed method is a type of topology optimization method since topological changes occur during the optimization procedure, such as the introduction of holes

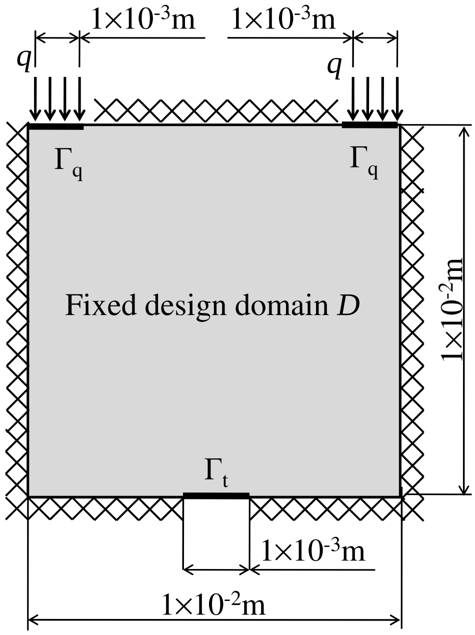

Figure 7.1: Fixed design domain and boundary conditions of the heat conduction problem

in Case 1, and changes in the number of holes in Cases 2 and 3. In addition, the obtained optimal configurations are clear, smooth and nearly the same, indicating that a clear and smooth optimal configuration can be obtained regardless of the initial configuration for the cases here.

7.3.2 Internal heat generation problem

Second, I consider an internal heat generation problem. Figure 7.3 shows the fixed design domain and boundary conditions. As shown, a central segment of the top line of the fixed design domain has a prescribed temperature of $25°C$. In addition, an internal heat generation output of 1.0×10^{-7}W/m^2 is uniformly applied over the fixed deign domain. The fixed design domain is discretized into four-node elements whose length is 2.5×10^{-5}m. The upper limit of the volume constraint $V_{\max}$ is set to 40% of the fixed design domain. Parameter K is set to 1, parameter c is set to 0.5 and the characteristic length L is set to 1×10^{-2}m. I shall examine how various values

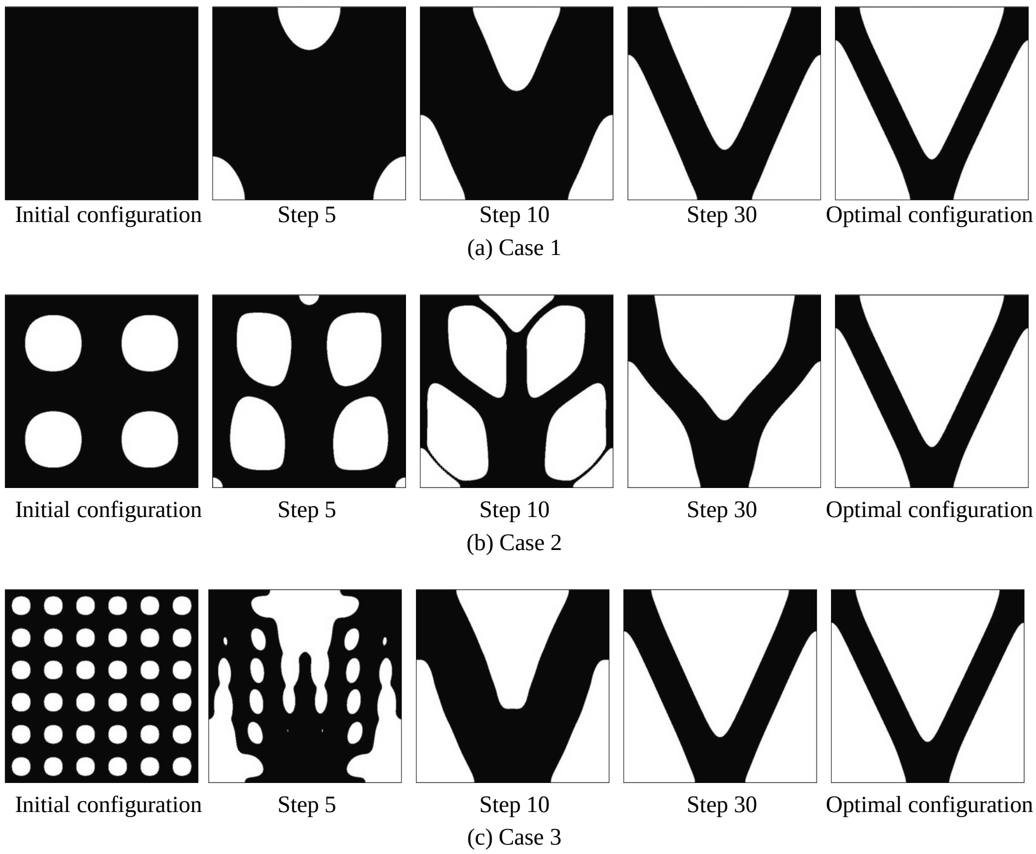

Figure 7.2: Configurations of the heat conduction problem: (a) Initial configuration with no holes; (b) Initial configuration with four holes; (c) Initial configuration with many holes.

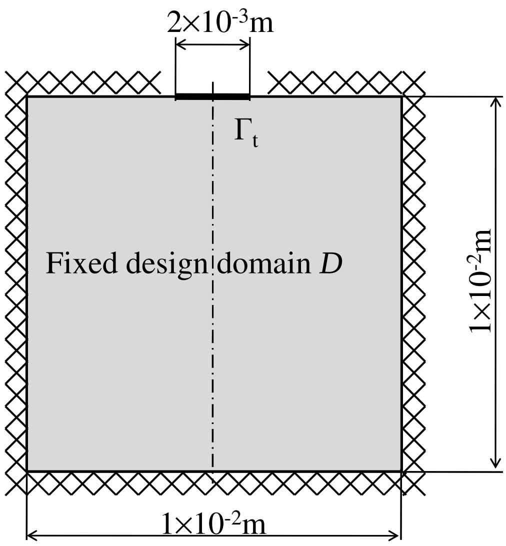

Figure 7.3: Fixed design domain and boundary conditions of the internal heat generation problem.

of the regularization parameter τ affect the resulting optimal configurations. The regularization parameter τ settings for the cases are Case 1: $\tau = 1.0 \times 10^{-6}$; Case 2: $\tau = 5.0 \times 10^{-6}$; Case 3: $\tau = 1.0 \times 10^{-5}$ and Case 4: $\tau = 5.0 \times 10^{-5}$. Figure 7.4 shows the optimal configurations of these cases. In all cases, fin shapes extended from the boundary Γ_t in order to diffuse the internal heat from the fixed design domain. The width of the fin shapes are thickest in the neighborhood of the boundary Γ_t, effectively conducting heat there, indicating that the obtained optimal configurations can be considered reasonable and proper. Furthermore, all optimal configurations are again clear and smooth. It is observed that the proposed method yields optimal configurations that have different degrees of geometrical complexity in response to different set values of the regularization parameter τ.

7.3.3 Heat convection problem

Now I consider two- and three-dimensional heat convection problems that include design-dependent boundary conditions. Figure 7.5 shows the fixed design domain

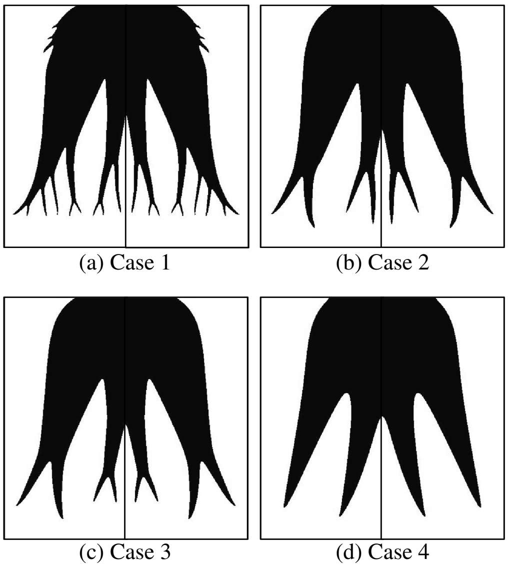

Figure 7.4: Optimal configurations of the internal heat generation problem: (a) Regularization parameter = 1.0×10^{-6}; (b) Regularization parameter = 5.0×10^{-6}; (c) Regularization parameter = 1.0×10^{-5}; (d) Regularization parameter = 5.0×10^{-5}.

and boundary conditions of the two-dimensional heat convection problem. As shown, the curved segment at the lower left of the fixed design domain has a prescribed temperature of 50°C. In addition, I impose design-dependent heat convection boundary conditions on the structural boundaries. That is, a heat convection load consisting of heat convection coefficient $h = 100$W/m·K and ambient temperature $T_{amb} = 25°C$ is set over the entire fixed design domain. The fixed design domain is discretized into four-node elements whose average length is 3.5×10^{-5}m. The upper limit of the volume constraint $V_{\max}$ is set to 40% of the fixed design domain. Parameter K is set to 1, parameter c is set to 0.5 and the characteristic length L is set to 1×10^{-2}m. First, I examine how different values of the regularization parameter τ affect the resulting optimal configurations. The regularization parameter τ settings for the cases are Case 1: $\tau = 1.0 \times 10^{-6}$; Case 2: $\tau = 5.0 \times 10^{-6}$; Case 3: $\tau = 1.0 \times 10^{-5}$ and Case 4: $\tau = 5.0 \times 10^{-5}$. Figure 7.6 shows the optimal configurations of these cases. It can be confirmed that appropriate fin shapes appear and maximize the heat con-

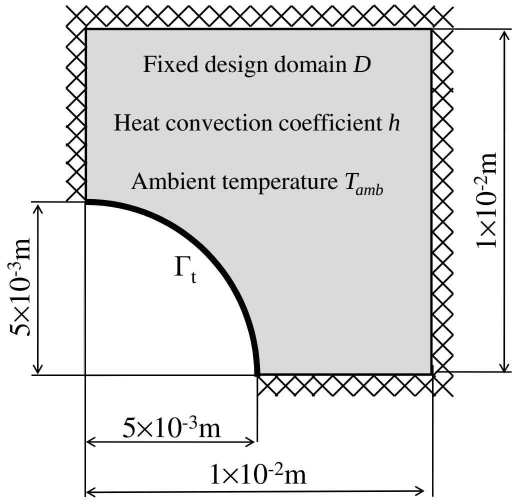

Figure 7.5: Fixed design domain and boundary conditions of the two-dimensional heat convection problem

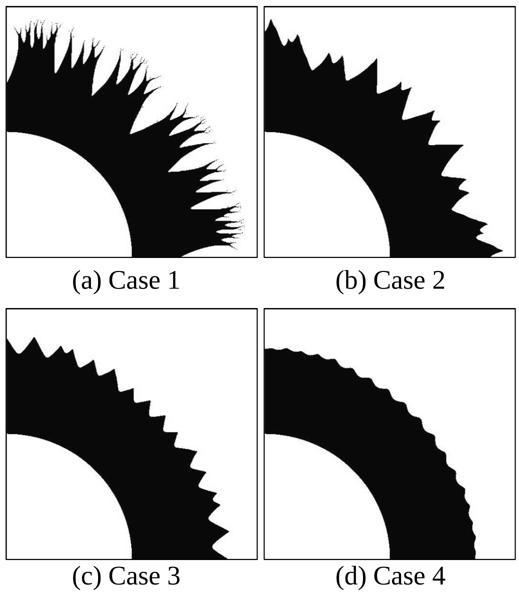

Figure 7.6: Optimal configurations of two-dimensional heat convection problem, considering shape dependencies with respect to regularization parameter τ: (a) Regularization parameter $= 1.0 \times 10^{-6}$; (b) Regularization parameter $= 5.0 \times 10^{-6}$; (c) Regularization parameter $= 1.0 \times 10^{-5}$; (d) Regularization parameter $= 5.0 \times 10^{-5}$.

vection effect from the structural boundaries of the optimal configurations. For cases requiring maximal thermal diffusivity by heat conduction, the optimal configurations should be free of holes, so I again confirm that the obtained optimal configurations can be considered reasonable and proper. In addition, all optimal configurations are clear and smooth. It is observed that the proposed method yields optimal configurations that have different degrees of geometrical complexity, in response to different set values of the regularization parameter τ.

Next, I examine how different values of the heat convection coefficient h affect the resulting optimal configurations. The regularization parameter is set to $\tau = 1.0 \times 10^{-5}$ for all cases. The heat convection coefficient h settings for the cases are Case 1: $h = 1.0 \times 10^5$; Case 2: $h = 2.0 \times 10^4$; Case 3: $h = 1.0 \times 10^4$ and Case 4: $h = 1.0 \times 10^2$. Figure 7.7 shows the optimal configurations for these cases and I again observe that fin shapes appear. The optimal configurations here show

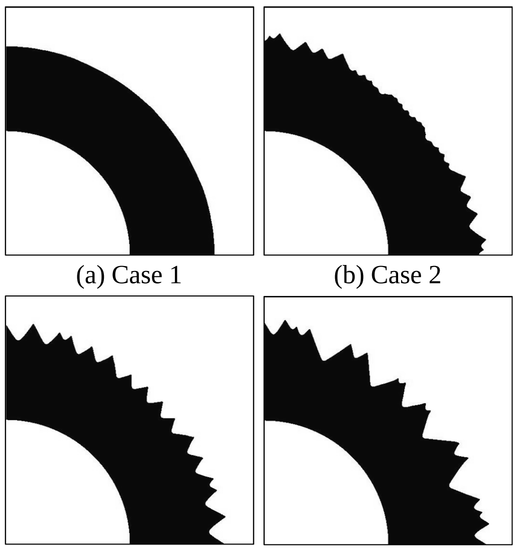

(a) Case 1 (b) Case 2 (c) Case 3 (d) Case 4

Figure 7.7: Optimal configurations of two-dimensional heat convection problem, considering shape dependencies with respect to heat convection coefficient h: (a) Heat convection coefficient $= 1.0 \times 10^5$; (b) Heat convection coefficient $= 2.0 \times 10^4$; (c) Heat convection coefficient $= 1.0 \times 10^4$; (d) Heat convection coefficient $= 1.0 \times 10^2$.

that lower heat convection coefficients tend to increase the length of heat convection boundary Γ_h and higher heat convection coefficients tend to minimize the distance between the temperature prescribed boundary Γ_t and heat convection boundary Γ_h. Therefore, when considering design-dependent heat convection loads, it is important to recognize that the optimal configurations are strongly influenced by the value of the heat convection coefficient.

Last, I consider a three-dimensional case and Figure 7.8 shows the fixed design domain and boundary conditions. The fixed design domain has a prescribed temperature of 80°C on boundary Γ_t. In addition, I impose design-dependent heat convection boundary conditions on the structural boundaries, where a heat convection load consisting of heat convection coefficient $h = 1 \times 10^3 \mathrm{W/m^2K}$ and ambient temperature $T_{amb} = 25°C$ is set over the entire fixed design domain. The fixed design domain is discretized into eight-node elements whose average length is 5×10^{-4}m. The upper limit of the volume constraint $V_{\max}$ is set to 50% of the fixed design domain. Parameter K is set to 1, parameter c is set to 0.5 and the characteristic length L is set to 1×10^{-2}m and the regularization parameter has $\tau = 1.0 \times 10^{-5}$. Figure 7.8 shows the obtained optimal configuration, which is smooth and clear.

7.4 Conclusions

It was constructed that a new level set-based topology optimization method for thermal problems, and achieved the following: First of all, a new level set-based topology optimization method that can deal with design-dependent boundary conditions was constructed, based on level set boundary expressions. The optimization problem for generic thermal problems was formulated using the concept of total potential energy and the sensitivities were derived based on the formulation and adjoint variable method. Finally, the numerical examples presented confirmed that the proposed method yields clear and smooth optimal configurations for structural designs consid-

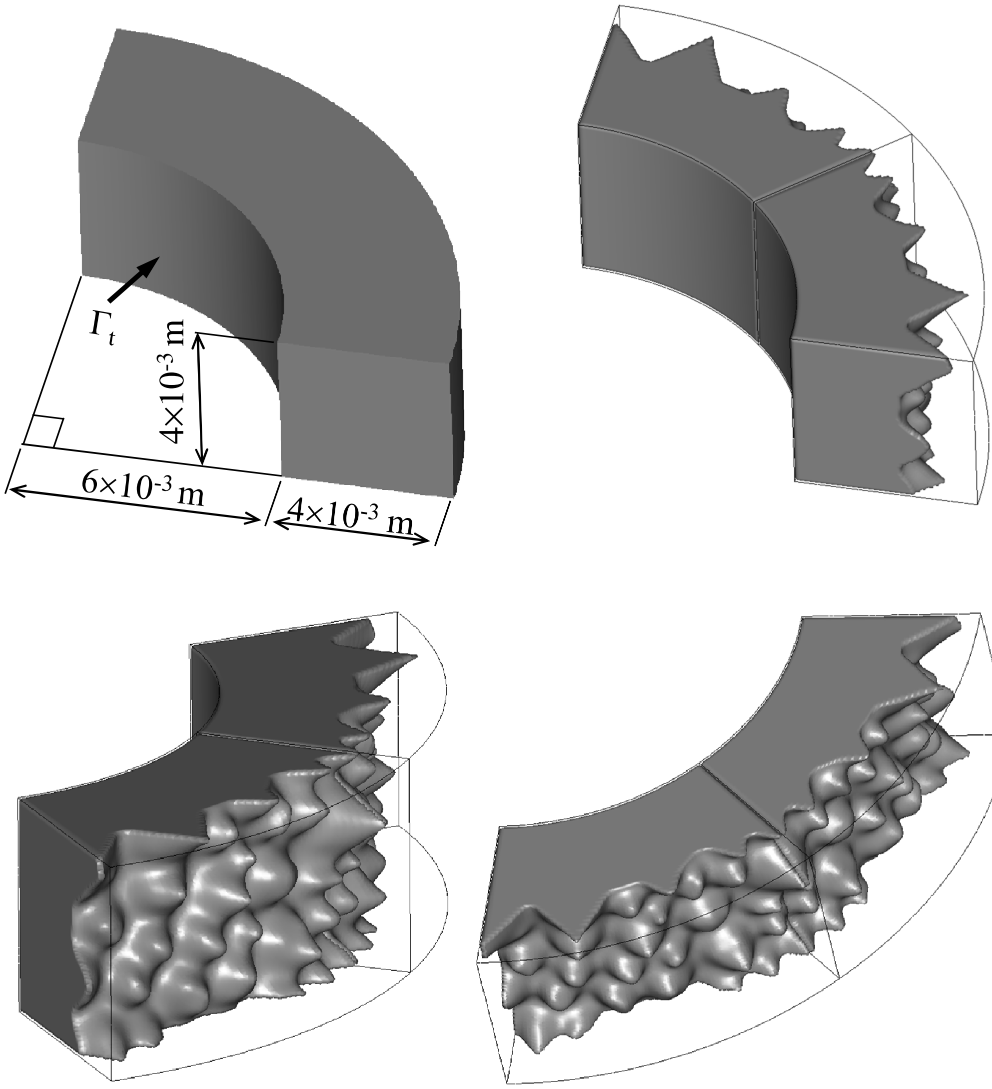

Figure 7.8: Fixed design domain and optimal configurations of three-dimensional heat convection problem.

ering heat conduction, internal heat generation and heat convection, and that the geometrical complexity of the optimal structures can be qualitatively specified by changing regularization parameter τ in the formulation of the objective functional.

Chapter 8

Conclusions

This thesis proposed a new topology optimization method incorporating level set boundary expressions based on the concept of the phase field method and applied it to minimum mean compliance problems, optimum compliant mechanism design problems, lowest eigenfrequency maximization problems and thermal problems. I achieved the following:

(1) A new topology optimization method was formulated, incorporating level set boundary expressions, where the optimization problem is handled as a problem to minimize the energy functional including a fictitious interface energy. Furthermore, a new method for solving the optimization problem using a reaction-diffusion equation was proposed.

(2) Based on the proposed topology optimization method, minimum mean compliance problems, optimum design problem of compliant mechanisms, lowest eigenfrequency maximization problems and thermal problems were formulated, and an optimization algorithm was then constructed. A scheme for updating the level set function using a time evolutional equation was proposed.

(3) Several numerical examples were provided to confirm the usefulness of the proposed topology optimization method for the various problems examined in this thesis.

It was confirmed that smooth and clear optimal configurations were obtained using the proposed topology optimization method, which also allows control of the geometrical complexity of the obtained optimal configurations. The obtained optimal configurations show minimal dependency upon the finite element size or initial configurations. In addition, we showed that uniform cross-section surface constraints can easily be imposed by using an anisotropic variation of the regularization parameter τ.

References

[1] Svanberg, K., Optimal geometry in truss design, in foundations of structural optimization: A unified approach, Wiley, New York, (1982).

[2] Prager, W., A note on discretized michell structures, *Computer Methods in Applied Mechanics and Engineering*, Vol.3, (1974), pp.349.

[3] Zienkiewicz, O. C. and Campbell, J. S., Shape optimization and sequential linear programming, in optimum structural design, Wiley, New York, (1973).

[4] Haslinger, J. and Mälinen, R. A. E., Introduction to shape optimization: Theory, approximation and computation, SIAM, Philadelphia, (2003).

[5] Mohammadi, B. and Pironneau, O., Applied shape optimization for fluids, Oxford University Press, Oxford, (2001).

[6] Pironneau, O., Optimal shape design for elliptic systems, Springer-Verlag, New York, (1984).

[7] Sokolowski, J. and Zolesio, J. P., Introduction to shape optimization: Shape sensitivity analysis, Springer-Verlag, Berlin, (1992).

[8] Bendsøe, M. P. and Kikuchi, N., Generating optimal topologies in structural design using a homogenization method, *Computer Methods in Applied Mechanics and Engineering*, Vol.71, (1988), pp.891–909.

[9] Bendsøe, M. P. and Sigmund, O., Topology optimization: Theory, methods, and applications, Springer-Verlag, Berlin, (2003).

[10] Cherkaev, A., Variational methods for structural optimization, Springer-Verlag, New York, (2000).

[11] Allaire, G., Shape optimization by the homogenization method, Springer-Verlag, (2002), pp.189–254.

[12] Suzuki, K. and Kikuchi, N., A homogenization method for shape and topology optimization, *Computer Methods in Applied Mechanics and Engineering*, Vol.121, (1991), pp.291–318.

[13] Diaz, A. R. and Kikuchi, N., Solutions to shape and topology eigenvalue optimization problems using a homogenization method, *International Journal for Numerical Methods in Engineering*, Vol.35, (1992), pp.1487–1502.

[14] Ma, D. and Kikuchi, N., Topological design for vibrating structures, *Computer Methods in Applied Mechanics and Engineering*, Vol.121, (1995), pp.259–280.

[15] Yang, X. Y., Xie, Y. M., Steven, G. P., and Querin, O. M., Topology optimization for frequencies using an evolutionary method, *Journal of Structural Engineering*, Vol.125, (1999), pp.1432–1438.

[16] Nishiwaki, S., Frecker, M. I., Min, S., and Kikuchi, N., Topology optimization of compliant mechanisms using the homogenization method, *International Journal for Numerical Methods in Engineering*, Vol.42, (1998), pp.535–559.

[17] Sigmund, O., On the design of compliant mechanisms using topology optimization, *Mechanics Based Design of Structures and Machines*, Vol.25, (1997), pp.493–524.

[18] Haslinger, J., Hillebrand, A., Karkkainen, T., and Miettinen, M., Optimization of conducting structures by using the homogenization method, *Structural and Multidisciplinary Optimization*, Vol.24, (2002), pp.125–140.

[19] Li, Q., Steven, G. P., Querin, O. M., and Xie, Y. M., Shape and topology design for heat conduction by evolutionary structural optimization, *International Journal of Heat and Mass Transfer*, Vol.42, (1999), pp.3361–3371.

[20] Iga, A., Nishiwaki, S., Izui, K., and Yoshimura, M., Topology optimization for thermal conductors with heat cpnvection and conduction including design-dependent effects, *International Journal of Heat and Mass Transfer*, Vol.52, (2009), pp.2721–2732.

[21] Murat, F. and Tartar, L., Optimality conditions and homogenization, *Proceedings of Nonlinear Variational Problems*, Vol.71, (1985), pp.1–8.

[22] Benssousan, A., Lions, J. L., and Papanicoulau, G., Asymptotic analysis for periodic structures, North-Holland, Amsterdam-New York-Oxford, (1978).

[23] Sanchez-Palencia, E., Non homogeneous media and vibration theory, lecture notes in physics 127, Springer-Verlag, Berlin, (1980).

[24] Lions, J. L., Some methods in mathematical analysis of systems and their control, Beijing, Kexue Chubanshe Science Press and Gordon & Breach Science Pub., (1981).

[25] Bendsøe, M. P., Optimal shape design as a material distribution problem, *Structural Optimization*, Vol.1, (1989), pp.193–202.

[26] Bendsøe, M. P. and Sigmund, O., Optimization of structural topology, shape and material, Springer, Berlin, (1997).

[27] Yang, R. J. and Chung, C. H., Optimal topology design using linear programming, *Computers and Structures*, Vol.53, (1994), pp.265–275.

[28] Bendsøe, M. P. and Sigmund, O., Material interpolation schemes in topology optimization, *Archive of Applied Mechanics*, Vol.69, (1999), pp.635–654.

[29] Cahn, J. W. and Hilliard, J. E., Free energy of a nonuniform system. i. interfacial free energy, *The Journal of Chemical Physics*, Vol.28, (1958), pp.258–267.

[30] Allen, S. M. and Cahn, J. W., A microscopic theory for antiphase boundary motion and its application to antiphase domain coarsening, *Acta Metall*, Vol.27, (1979), pp.1085–1095.

[31] Eyre, D., Systems of cahn-hilliard equations, *SIAM Journal on Applied Mathematics*, Vol.53, No.6, (1993), pp.1686–1712.

[32] Leo, P. H., Lowengrub, J. S., and Jou, H. J., A diffuse interface model for microstructural evolution in elastically stressed solids, *Acta Metall*, Vol.46, No.6, (1998), pp.2113–2130.

[33] Wang, M. Y. and W., Z. S., Phase field: A variational method for structural topology optimization, *Computer Modeling in Engineering and Sciences*, Vol.6, No.6, (2004), pp.547–566.

[34] Zhou, S. and Wang, M. Y., Multimaterial structural topology optimization with a generalized cahn-hilliard model of multiphase transition structural and multidisciplinary optimization, *Structural and Multidisciplinary Optimization*, Vol.33, No.2, (2007), pp.89–111.

[35] Zhou, S. and Wang, M. Y., 3d multi-material structural topology optimization with the generalized cahn-hilliard equations, *Computer Modeling in Engineering and Science*, Vol.16, No.2, (2006), pp.83–101.

[36] Wang, M. Y., Zhou, S., and Ding, H., Nonlinear diffusions in topology optimization, *Structural and Multidisciplinary Optimization*, Vol.28, (2004), pp.262–276.

[37] Wang, M. Y. and Zhou, S., Synthesis of shape and topology of multi-material structures with a phase-field method, *Journal of Computer-Aided Materials Design*, Vol.11, (2004), pp.117–138.

[38] Burger, M. and Stainko, R., Phase-field relaxation of topology optimization with local stress constraints, *SIAM Journal on Control and Optimization*, Vol.45, No.4, (2006), pp.1447–1466.

[39] Xie, Y. M. and Steven, G. P., A simple evolutionary procedure for structural optimization, *Computers and Structures*, Vol.49, (1993), pp.885–896.

[40] Diaz, A. Z. and Sigmund, O., Checkerboard patterns in layout optimization, *Structural Optimization*, Vol.10, (1995), pp.40–45.

[41] Sigmund, O. and Petersson, J., Numerical instabilities in topology optimization: A survey on procedures dealing with checkerboards, mesh-dependencies and local minima, *Structural Optimization*, Vol.16, (1998), pp.68–75.

[42] Haber, R. B., Jog, C. S., and Bendsøe, M. P., A new approach to variable-topology shape design using a constraint on perimeter, *Structural and Multidisciplinary Optimization*, Vol.11, (1996), pp.1–12.

[43] Petersson, J. and Sigmund, O., Slope constrained topology optimization, *International Journal for Numerical Methods in Engineering*, Vol.41, No.8, (1998), pp.1417–1434.

[44] Zhou, M., Shyy, Y. K., and Thomas, H. L., Checkerboard and minimum member size control in topology optimization method, *Structural and Multidisciplinary Optimization*, Vol.21, No.2, (2001), pp.152–158.

[45] Osher, S. and Sethian, J. A., Front propagating with curvature dependent speed: Algorithms based on the hamilton-jacobi formulations, *Journal of Computational Physics*, Vol.78, (1988), pp.12–49.

[46] Sussman, M., Smereka, P., and Osher, S., A level set approach for computing solutions to incompressible two-phase flow, *Journal of Computational Physics*, Vol.114, (1994), pp.146–159.

[47] Chang, Y. C., Hou, T. Y., Merriman, B., and Osher, S., A level set formulation of eulerian interface capturing methods for incompressible fluid flow, *Journal of Computational Physics*, Vol.124, (1996), pp.449–464.

[48] Susmman, M. and Puckett, E. G., A coupled level set and volume-of-fluid method for computing 3d and axisymmetric incompressible two-phase flows, *Journal of Computational Physics*, Vol.162, (2000), pp.301–337.

[49] Son, G. and Dhir, V. K., Numerical simulation of film boiling near critical pressures with a level set method, *Journal of Heat Transfer*, Vol.120, (1998), pp.183–192.

[50] Ye, J. C., Bresler, Y., and Moulin, P., A self-referencing level-set method for image reconstruction from sparse fourier samples, *International Journal of Computer Vision*, Vol.50, (2002), pp.253–270.

[51] Tsai, R. and Osher, S., Level set methods and their applications in image science, *Communications in Mathematical Sciences*, Vol.1, (2003), pp.623–656.

[52] Doel, K. and Ascher, U. M., On level set regularization for highly ill-posed distributed parameter estimation problems, *Journal of Computational Physics*, Vol.216, (2006), pp.707–723.

[53] Sethian, J. A., Level set method and fast marching methods, Cambridge Monographs on Applied and Computational Mechanics (2nd edn), Cambridge University Press, Cambridge, U. K., (1999).

[54] Sethian, J. A. and Wiegmann, A., A structural boundary design via level-set and immersed interface methods, *Journal of Computational Physics*, Vol.163, (2000), pp.489–528.

[55] Osher, S. and Santosa, F., Level-set methods for optimization problems involving geometry and constraints: Frequencies of a two-density inhomogeneous drum, *Journal of Computational Physics*, Vol.171, (2001), pp.272–288.

[56] Belytschko, T., Xiao, S. P., and Parimi, C., Topology optimization with implicit functions and regularization, *International Journal for Numerical Methods in Engineering*, Vol.57, (2003), pp.1177–1196.

[57] Wang, M. Y., Wang, X., and Guo, D., A level set method for structural topology optimization, *Computer Methods in Applied Mechanics and Engineering*, Vol.192, (2003), pp.227–246.

[58] Wang, M. Y. and Wang, X., "color" level sets: a multi-phase method for structural topology optimization with multiple materials, *Computer Methods in Applied Mechanics and Engineering*, Vol.193, (2004), pp.469–496.

[59] Allaire, G., Jouve, F., and Toader, A., Structural optimization using sensitivity analysis and a level-set method, *Journal of Computational Physics*, Vol.194, (2004), pp.363–393.

[60] Allaire, G. and Jouve, F., A level-set method for vibration and multiple loads structural optimization, *Computer Methods in Applied Mechanics and Engineering*, Vol.194, (2005), pp.3269–3290.

[61] Leitao, A. and Scherzer, O., On the relation between constraint regularization, level sets and shape optimization, *Inverse Problems*, Vol.19, (2003), pp.1–11.

[62] Chen, J., Shapiro, V., and Tsukanov, K. I., Shape optimization with topological changes and parametric control, *International Journal for Numerical Methods in Engineering*, Vol.71, (2007), pp.313–346.

[63] Wang, S. Y. and Wang, M. Y., A moving superimposed finite element method for structural topology optimization, *International Journal for Numerical Methods in Engineering*, Vol.65, (2006), pp.1892–1922.

[64] Wei, P. and Wang, M. Y., Piecewise constant level set method for structural topology optimization, *International Journal for Numerical Methods in Engineering*, Vol.78, No.4, (2008), pp.379–402.

[65] Luo, Z., Tong, L., Luo, J., Wei, P., and Wang, M. Y., Design of piezoelectric actuators using a multiphase level set method of piecewise constants, *Journal of Computational Physics*, Vol.228, (2009), pp.2643–2659.

[66] Luo, Z., Tong, L., and Ma, H., Shape and topology optimization for electrothermomechanical microactuators using level set methods, *Journal of Computational Physics*, Vol.228, (2009), pp.3173–3181.

[67] Park, S. and Min, S., Magnetic actuator design for maximizing force using level set based topology optimization, *IEEE transactions on magnetics*, Vol.45, No.5, (2009), pp.2336–2339.

[68] Shim, H., Ho, V. T. T., Wang, S., and Tortorelli, D. A., Topological shape optimization of electromagnetic problems using level set method and radial basis function, *Computer Moldering in Engineering and Scienceg*, Vol.37, No.2, (2008), pp.175–202.

[69] Yamada, T., Yamasaki, S., Nishiwaki, S., Izui, K., and Yoshimura, M., Design of compliant thermal actuator using structural optimization based on the level set method, *Transactions of the ASME, Journal of Computing And Information Science In Engineering, (submitted).*

[70] Allaire, G., Gournay, F., Jouve, F., and Toader, A. M., Structural optimization using topological and shape sensitivity via a level set method, *Internal Report 555, Ecole Polytechnique, France*, (2004).

[71] Eschenauer, H. A., Kobelev, V., and Schumacher, A., Bubble method for topology and shape optimization of structures, *Structural Optimization*, Vol.8, (1994), pp.42–51.

[72] Sokolowski, J. and Zochowski, A., On the topological derivatives in shape optimization, *SIAM Journal on Control and Optimization*, Vol.37, (1999), pp.1251–1272.

[73] He, L., Kao, C. Y., and Osher, S., Incorporating topological derivatives into shape derivatives based level set methods, *Journal of Computational Physics*, Vol.225, (2007), pp.891–909.

[74] Novotny, A. A., Feijóo, R. A., Taroco, E., and Padra, C., Topological sensitivity analysis, *Computer Methods in Applied Mechanics and Engineering*, Vol.192, (2003), pp.803–829.

[75] Wang, S. Y., Lim, K. M., Khoo, B. C., and Wang, M. Y., An extended level set method for shape and topology optimization, *Journal of Computational Physics*, Vol.221, (2007), pp.395–421.

[76] Chopp, D. L., Computing minimal surfaces via level set curvature flow, *Journal of Computational Physics*, Vol.106, (1993), pp.77–91.

[77] Wang, S. Y. and Wang, M. Y., Radial basis functions and level set method for structural topology optimization, *International Journal for Numerical Methods in Engineering*, Vol.65, (2006), pp.2060–2090.

[78] Yamasaki, S., Nishiwaki, S., Yamada, T., Izui, K., and Yoshimura, M., A structural optimization method based on the level set method using a new geometry-based re-initialization scheme, *International Journal for Numerical Methods in Engineering, (submitted).*

[79] Tikhonov, A. N. and Arsenin, V. Y., Solutions of ill-posed problems, Winston and Sons, Washington, D. C., (1997).

[80] Braides, A., Γ-convergence for beginners, Oxford Lecture Series In Mathematics and Its Applications 22, Oxford University Press, Oxford, (2002).

[81] He, L., Kao, C. Y., and Osher, S., Incorporating topological derivatives into shape derivatives based level set methods, *Journal of Computational Physics*, Vol.225, (2007), pp.891–909.

[82] Novotny, A. A., Feijóo, R. A., Taroco, E., and Padra, C., Topological sensitivity analysis, *Computer Methods in Applied Mechanics and Engineering*, Vol.192, (2003), pp.803–829.

[83] Hestenes, M. R., Multiplier, gradient methods, *Journal of Optimization Theory and Applications*, Vol.4, No.5, (1969), pp.303–320.

[84] Powell, M., A method for nonlinear constraints in minimization problems, *Optimization, Academic Press, London, England*, (1969), pp.283–298.

[85] Rockafellar, R. T., The multiplier method of hestenes and powell applied to convex programming, *Journal of Optimization Theory and Applications*, Vol.12, (1973), pp.555–562.

[86] Ananthasuresh, G. K. and Moulton, T., Micromechanical devices with embedded electro-thermal-compliant actuation, *Sensors and Actuators A*, Vol.90, (2001), pp.38–48.

[87] Prasanna, S. and Spearing, S. M., Materials selection and design of microelectrothermal bimaterial actuators, *Journal of Microelectromechanical Systems*, Vol.16, (2007), pp.248–259.

[88] Schweizer, S., S. Calmes, M. L., and Renaud, R., Thermaly actuated optimal microscanner with large angle and low consumption, *Sensors and Actuators*, Vol.76, (1999), pp.470–477.

[89] Pai, M. and Tien, N. C., Low voltage electrothermal vibromotor for silicon optical bench applications, *Sensors and Actuators*, Vol.83, (2000), pp.237–243.

[90] Kwon, H. N., Jeong, S. H., Lee, S. K., and Lee, J. H., Desgin and characterization of a micromachined inchworm motor with thermoelastic linkage actuators, *Sensors and Actuators A*, Vol.103, (2003), pp.143–149.

[91] Setevenson, M., Yang, P., Lai, Y., and Mechefske, C., Development of a bidirectional ring thermal actuator, *Journal of Micromechanics and Microengineering*, Vol.17, (2007), pp.2049–2054.

[92] Que, L., Park, J. S., and Gianchandani, Y. B., Bent-beam electrothermal actuators - part i: Single beam and cascaded deviced, *Journal of Microelectromechanical Systems*, Vol.10, (2001), pp.247–254.

[93] Park, J. S., Chu, A. D., and Gianchandani, Y. B., Bent-beam electrothermal actuators - part ii: Linear and rotary microengines, *Journal of Microelectromechanical Systems*, Vol.10, (2001), pp.255–262.

[94] Chen, R. S., Kung, C., and Lee, G. B., Analysis of the optimal dimension on the electrothermal microactuator, *Institute of Physics Publishing*, Vol.12, (2002), pp.291–296.

[95] Wang, Y., Li, Z., Mccormick, D. T., and Tien, N. C., A micromachined rf microrelay with electrothermal actuation, *Sensors and Actuators A*, Vol.103, (2003), pp.231–236.

[96] Yoon, G. H., Kim, Y. Y., Bendsøe, M. P., and Sigmund, O., High-free topology optimization with embedded translation-invariant differentiable wavelet srhinkage, *Structural and Multidisciplinary Optimization*, Vol.27, (2004), pp.139–150.

[97] Duysinx, P. and Bendsøe, M. P., Topology optimization of continuum structures with local stress constraints, *International Journal for Numerical Methods in Engineering*, Vol.43, (1998), pp.1453–1478.

[98] Silva, E. C. N., Fonseca, J. S. O., and Kikuchi, N., Optimal design of piezoelectric microstructures, *Journal of Computational Mechanics*, Vol.19, (1997), pp.397–410.

[99] Jose, K. A., Suh, W. D., Xavier, P. B., Varadan, V. K., and Varadan, V. V., Surface acoustic wave MEMS gyroscope, *Wave Motion*, Vol.36, (2002), pp.367–381.

[100] Saitou, K., Wang, D. A., and Wou, S. J., Externally resonated linear mocrovibromotor for microassembly, *Journal of Microelectromechanical System*, Vol.9, (2000), pp.336–346.

[101] Gao, T., Zhang, W., Zhu, J., and Xu, Y., Topology optimization of heat conduction problem involving design-dependent effect, in *Proceedings of the Forth China-Japan Korea Joint Symposium on Structural and Mechanical Systems*, (2006).

[102] Yoon, G. H. and Kim, Y. Y., The element connectivity parameterization formulation for the topology design optimization of multiphysics system, *International Journal for Numerical Methods in Engineering*, Vol.64, (2005), pp.1649–1677.

[103] Chen, B. C. and Kikuchi, N., Topology optimization with design-dependent loads, *Finite Elements Analysis Design*, Vol.37, (2001), pp.57–70.

About the author

Takayuki Yamada was born in Gifu City, Japan, on April 25, 1984.

From April 2000 to March 2005, he received special technical education in mechanical engineering at Gifu National College of Technology (GNCT) in Motosu City, Gifu Prefecture. There, he first studied basic optimum design concepts with Professor Eiji Katamine and became interested in working in the optimum design field. His graduation research topic was "Crystal Growth of Ultrafine Au-Pb Particles Prepared by a Gas-Evaporation Technique".

From April 2005 to March 2007, he received his undergraduate education in engineering science at Kyoto University in Kyoto City, Japan. He joined the fluid dynamics laboratory headed by Professor Inamuro in the Department of Aeronautics and Astronautics. The title of his bachelor's thesis was "Rarefied Gas Flow Induced by a Mesh Pair at Different Temperatures". For this research, he designed and built the experimental systems, based on his experience at GNCT. In 2007, he received his B.A. in Engineering from Kyoto University.

In March 2008, he received his M.A. in Engineering from Kyoto University. The title of his masters thesis was "Structural Optimization of Functional Structures Based on the Level Set Method". This research topic dealt with a type of shape optimization method based on the level set method and successfully extended a level set-based structural optimization method to multiphysics problems.

After receiving his M.A. degree, he entered a doctoral course at Kyoto University.

In April 2008, he decided on the topics covered in this thesis, based on his prior and ongoing research experience. In April 2009, he became a research fellow of the Japan Society for the Promotion of Science. In the summer of 2009, using a JSPS grant for fellows, he worked at the Laboratory of Professor Alejandro R. Diaz at Michigan State University for a month as a visiting scholar. In the course of his masters and doctoral studies, he has published many journal papers, given numerous research presentations at domestic and international conferences, and has received a number of awards, such as the JSME Best Paper Prize in April 2010.

List of Publications

Journal Papers

[1] Takayuki Yamada, Shintaro Yamasaki, Shinji Nishiwaki, Kazuhiro Izui and Masataka Yoshimura, Structural Optimization of Compliant Mechanisms Based on the Level Set Method, *Transactions of Japan Society for Computational Engineering and Science*, Vol. 2008, Paper No. 20080001, 2008. (In Japanese)

[2] Takayuki Yamada, Shintaro Yamasaki, Shinji Nishiwaki, Kazuhiro Izui and Masataka Yoshimura, Structural Optimization of Compliant Thermal Actuators Based on the Level Set Method, *Transactions of Japan Society for Computational Engineering and Science*, Vol. 2008, Paper No. 20080007, 2008. (In Japanese)

[3] Takayuki Yamada, Shintaro Yamasaki, Shinji Nishiwaki, Kazuhiro Izui and Masataka Yoshimura, A Study of Boundary Settings in the Design Domain for Structural Optimization Based on the Level Set Method, *Transactions of the Japan Society for Industrial and Applied Mathematics*, Vol. 18, No. 3, 2008, pp.487-505. (In Japanese)

[4] Shintaro Yamasaki, Shinji Nishiwaki, Takayuki Yamada, Kazuhiro Izui and Masataka Yoshimura, A Structural Optimization Method Based on the Level Set Method Using a New Geometry-Based Re-initialization Scheme, *International Journal for Numerical Methods in Engineering*, (accepted).

[5] Takayuki Yamada, Shinji Nishiwaki, Kazuhiro Izui, Masataka Yoshimura and Akihiro Takezawa, A Structural Optimization Method Incorporating Level Set Boundary Expressions Based on the Concept of the Phase Field Method, *Transactions of the Japan Society of Mechanical Engineers. A*, Vol. 75, No. 753, 2009, pp.550-558. (In Japanese)

[6] Yuji Okamoto, Kazuhiro Izui, Aturo Iga, Takayuki Yamada, Shinji Nishiwaki and Masataka Yoshimura, Topology Optimization for Thermal Problems Considering Thermoelectric Effect, *Transactions of Japan Society for Computational Engineering and Science*, Vol. 2009, Paper No. 20090005, 2009. (In Japanese)

[7] Takayuki Yamada, Shintaro Yamasaki, Shinji Nishiwaki, Kazuhiro Izui and Masataka Yoshimura, Design of Compliant Thermal Actuators Using Structural Optimization Based on the Level Set Method, *Transaction of ASME, Journal of Computing and Information Science in Engineering*, (submitted).

[8] Takayuki Yamada, Aturo Iga, Shinji Nishiwaki, Kazuhiro Izui, and Masataka Yoshimura, Level set-based topology optimization method for thermal problems, *Transactions of the Japan Society of Mechanical Engineers. C*, Vol. 75, No. 759, 2009, pp.2868-2876. (In Japanese)

[9] Yutaka Hirano, Takayuki Yamada, Nozomu Kogiso and Shinji Nishiwaki, Reliability-Based Topology Optimization Incorporating Level Set Boundary Expressions, *Transactions of the Japan Society of Mechanical Engineers. C*, Vol. 75, No. 758, 2009, pp.2633-2648. (In Japanese)

[10] Shintaro Yamasaki, Tsuyoshi Nomura, Kazuo Sato, Shinji Nishiwaki, Takayuki Yamada and Kazuhiro Izui, A Level Set Method-based Topology Optimization Method Using the Discretization-based Sensitivity with Respect to the Signed Distance Function, *Transactions of Japan Society for Computational Engineering*

and Science, Vol. 2009, Paper No. 20090012, 2009. (In Japanese)

[11] Aturo Iga, Takayuki Yamada, Shinji Nishiwaki, Kazuhiro Izui and Masataka Yoshimura, Topology Optimization for Coupled Thermal and Structural Problems Using the Level Set Method, *Transactions of the Japan Society of Mechanical Engineers. C*, Vol. 76, No. 761, 2010, pp.36-43. (In Japanese)

[12] Takayuki Yamada, Kazuhiro Izui, Shinji Nishiwaki and Akihiro Takezawa, A Topology Optimization Method Based on the Level Set Method Incorporating a Fictitious Interface Energy, Computer Methods in Applied Mechanics and Engineering, (accepted).

[13] Yuji Okamoto, Takayuki Yamada, Kazuhiro Izui, Shinji Nishiwaki. and Akihiro Takezawa, Level Set Based Topology Optimization of Thermal Actuators Considering Thermoelectric Effects, *Transactions of Japan Society for Computational Engineering and Science*, Vol. 2009, Paper No. 20090024, 2009. (In Japanese)

[14] Takayuki Yamada, Kazuhiro Izui and Shinji Nishiwaki, Level Set-Based Topology Optimization Method for Maximizing Thermal Diffusivity Problems Including Design-Dependent Effect, *Transactions of the ASME, Journal of Mechanical Design*, (submitted).

[15] Masatoshi Manabe, Takayuki Yamada, Kazuhiro Izui and Shinji Nishiwaki, Topology Optimization Incorporating Level Set Boundary Expressions Using a Particle Method, *Transactions of the Japan Society of Mechanical Engineers. A*, (submitted).

[16] Takayuki Yamada, Kazuhiro Izui, Shinji Nishiwaki, Masashi Sato and Osamu Tabata, An Optimum Design Method for Capacitive Micromachined Ultrasonic Transducers (Level Set-Based Topology Optimization Method Incorporating Uniform Cross-Section Surface Constraints), *Transactions of the Japan Society of*

Mechanical Engineers. A, (submitted).

[17] Sughoon Lim, Takayuki Yamada, Seungjae Min and Shinji Nishiwaki, Topology Optimization of Magnetic Actuator Based on a Level-Set and a Phase-Field Approach, *IEEE Transactions on Magnetics*, (submitted).

Refereed International Proceedings

[1] Takayuki Yamada, Shinji Nishiwaki, Shintaro Yamasaki, Kazuhiro Izui and Masataka Yoshimura, Optimum Structural Design of Thermal Actuators Using the Level Set Method, *Proceedings of 5th China-Japan-Korea Joint Symposium on Optimization of Structural and Mechanical Systems (CJK-OSM5)* June 16-19, 2008, Jeju, South Korea, DT-J006.

[2] Yuji Okamoto, Kazuhiro Izui, Takayuki Yamada, Aturo Iga, Shinji Nishiwaki, Masataka Yoshimura and John E. Renaud, Topology Optimization of Heat Transfer Control Systems Using Thermoelectric Devices, *Proceedings of 5th China-Japan-Korea Joint Symposium on Optimization of Structural and Mechanical Systems (CJK-OSM5)*, June 16-19, 2008, Jeju, South Korea, ST4-J016.

[3] Takayuki Yamada, Shintaro Yamasaki, Shinji Nishiwaki, Kazuhiro Izui and Masataka Yoshimura, Design of Compliant Thermal Actuators Using Structural Optimization Based on the Level Set Method, *Proceedings of ASME 2008 International Design Engineering Technical Conferences & Computers and Information in Engineering Conference (IDETC/CIE 2008)*, August 3-6, 2008, Brooklyn, New York, USA, DETC2008-49618.

[4] Takayuki Yamada, Shintaro Yamasaki, Shinji Nishiwaki, Kazuhiro Izui and Masataka Yoshimura, Structural Optimization of the Compliant Thermal Micro Actuators Based on the Level Set Method, *Proceedings of 12th AIAA/ISSMO Multidisci-*

plinary Analysis and Optimization Conference (2008MAO), Structural and Topology Optimization(Invited Session), September 10-12, 2008, British Columbia, Canada, AIAA2008-5937.

[5] Shintaro Yamasaki, Shinji Nishiwaki, Takayuki Yamada, Kazuhiro Izui and Masataka Yoshimura, A New Optimization Method Based on the Level Set Method for Vibration Problems and Heat Conduction Problems, *Proceedings of 12th AIAA/ISSMO Multidisciplinary Analysis and Optimization Conference (2008MAO)*, September 10-12, 2008, British Columbia, Canada, AIAA2008-6082.

[6] Kazuko Fuchi, Alejandro R. Diaz, Takayuki Yamada and Shinji Nishiwaki, A Level Set-Based Topology Optimization Method for Power Flow Control in Electromagnetics, *Proceedings of 8th World Congress on Structural and Multidisciplinary Optimization (WCSMO-8)*, June 1-5, 2009, Lisbon, Portugal, No.1043.

[7] Takayuki Yamada, Shinji Nishiwaki, Kazuhiro Izui and Masataka Yoshimura, A New Level Set Based Topology Optimization Method Using a Fictitious Interface Energy Model Based on Phase Field Method Concepts, *Proceedings of 8th World Congress on Structural and Multidisciplinary Optimization (WCSMO-8)*, June 1-5, 2009, Lisbon, Portugal, No.1136.

[8] Yuji Okamoto, Takayuki Yamada, Aturo Iga, Kazuhiro Izui, Shinji Nishiwaki and Masataka Yoshimura, Topology Optimization for the Design of Compliant Thermal Actuators Using Thermoelectric Devices, *Proceedings of 8th World Congress on Structural and Multidisciplinary Optimization (WCSMO-8)*, June 1-5, 2009, Lisbon, Portugal, No.1198.

[9] Kazuhiro Izui, Shintaro Yamasaki, Shinji Nishiwaki, Takayuki Yamada and Masataka Yoshimura, Comparison of Conventional Re-initialization Techniques and Development of a New Geometry-Based Re-initialization Scheme for Use in Level

Set-Based Structural Optimization Methods, *Proceedings of 8th World Congress on Structural and Multidisciplinary Optimization (WCSMO-8)*, June 1-5, 2009, Lisbon, Portugal, No.1199.

[10] Yutaka Hirano, Takayuki Yamada, Nozomu Kogiso, Shinji Nishiwaki, Reliability-Based Topology Optimization Incorporating Level Set Boundary Expressions by Phase Field Method Concepts, *Proceedings of 8th World Congress on Structural and Multidisciplinary Optimization (WCSMO-8)*, June 1-5, 2009, Lisbon, Portugal, No.1283.

[11] Takayuki Yamada, Shinji Nishiwaki, Atsuro Iga, Kazuhiro Izui and Masataka Yoshimura, Level Set-Based Topology Optimization Method for Thermal Problems Considering Design-Dependent Boundary Effects, *Proceedings of ASME 2009 International Design Engineering Technical Conferences & Computers and Information in Engineering Conference (IDETC/CIE 2009)*, August 30-September 2, 2009, San Diego, CA, USA, DETC2009-86618.

[12] Kazuhiro Izui, Kiyoshi Yokota, Takayuki Yamada, Shinji Nishiwaki and Masataka Yoshimura, A Structural Optimization Method for Universal Design of Compliant Mechanism Scissors, *Proceedings of ASME 2009 International Design Engineering Technical Conferences & Computers and Information in Engineering Conference (IDETC/CIE 2009)*, August 30-September 2, 2009, San Diego, CA, USA, DETC2009-86594.

[13] Sughoon Lim, Takayuki Yamada, Seungjae Min and Shinji Nishiwaki, Topology Optimization of Magnetic Actuator Based on a Level-Set and a Phase Field Approach, *Proceedings of 14th Biennial IEEE Conference on Electromagnetic Field Computation,* May 9-12, 2010, Chicago Illinois, USA, CEFC2010-1103.

[14] Takayuki Yamada, Kazuhiro Izui and Shinji Nishiwaki, A Topology Optimization

Method Incorporating Geometric Constraints Using Level Set Boundary Expressions, *Proceedings of 5th China-Japan-Korea Joint Symposium on Optimization of Structural and Mechanical Systems (CJK-OSM5)*, June 22-25, 2010, Kyoto, JAPAN, (accepted).

[15] Lim Yi Kang, Yuji Okamoto, Takayuki Yamada, Kazuhiro Izui and Shinji Nishiwaki, Topology Optimization of Piezoelectric Devices Using the Level Set Method Incorporating Fictitious Interface Energy, *Proceedings of 5th China-Japan-Korea Joint Symposium on Optimization of Structural and Mechanical Systems (CJK-OSM5)*, June 22-25, 2010, Kyoto, JAPAN, (accepted).

[16] Masatoshi Manabe, Takayuki Yamada, Kazuhiro Izui and Shinji Nishiwaki, Level Set-Based Topology Optimization for Nonlinear Structural Problems Using a Particle Method, *Proceedings of 5th China-Japan-Korea Joint Symposium on Optimization of Structural and Mechanical Systems (CJK-OSM5)*, June 22-25, 2010, Kyoto, JAPAN, (accepted).

[17] Yutaka Hirano, Takayuki Yamada, Nozomu Kogiso, Shinji Nishiwaki and Atsuro Iga, Robust Topology Optimum Design for Coupled Thermal and Structural Problems Using Level Set Boundary Expressions, *Proceedings of 5th China-Japan-Korea Joint Symposium on Optimization of Structural and Mechanical Systems (CJK-OSM5)*, June 22-25, 2010, Kyoto, JAPAN, (accepted).

[18] Kotani Takayo, Takayuki Yamada, Kazuhiro Izui and Shinji Nishiwaki, Optimum Design of Compliant Actuators Using Level Set-Based Topology Optimization Method, *Proceedings of 5th China-Japan-Korea Joint Symposium on Optimization of Structural and Mechanical Systems (CJK-OSM5)*, June 22-25, 2010, Kyoto, JAPAN, (accepted).

[19] Takayuki Yamada, Kazuhiro Izui and Shinji Nishiwaki, A Shape and Topology

Optimization Method Incorporating Level Set Boundary Expressions for Vibration Problems, *Proceedings of 13th AIAA/ISSMO Multidisciplinary Analysis and Optimization Conference (2010MAO)*, September 13-15, 2010, Fort Worth, Texas, USA, (accepted).

[20] Masatoshi Manabe, Takayuki Yamada, Kazuhiro Izui, Shinji Nishiwaki, Level Set-Based Topology Optimization for Mechanical Structures with Large Deformation Using a Particle Method, *Proceedings of 13th AIAA/ISSMO Multidisciplinary Analysis and Optimization Conference (2010MAO)*, September 13-15, 2010, Fort Worth, Texas, USA, (accepted).

[21] Shintaro Yamasaki, Takayuki Yamada, Toru Matsushima, Kazuhiro Izui and Shinji Nishiwaki, A Level Set Based Topology Optimization Method Targeting Dynamic Characteristics of Rotational Symmetry Structures, *Proceedings of 13th AIAA/ISSMO Multidisciplinary Analysis and Optimization Conference (2010MAO)*, September 13-15, 2010, Fort Worth, Texas, USA, (accepted).

[22] Yutaka Hirano, Takayuki Yamada, Nozomu Kogiso, Shinji Nishiwaki and Atsuro Iga, Robust Design Using Level-Set Based Topology Optimization for Coupled Thermal and Structural Problems, *Proceedings of 13th AIAA/ISSMO Multidisciplinary Analysis and Optimization Conference (2010MAO)*, September 13-15, 2010, Fort Worth, Texas, USA, (accepted).

Non refereed International Proceedings

[1] Shintaro Yamasaki, Shinji Nishiwaki, Takayuki Yamada, Kazuhiro Izui and Masataka Yoshimura, Structural Optimization for Eigen-Frequency Problem Based on the Level Set Method, *Proceedings of The 7th International Conference on Optimization: Techniques and Applications (ICOTA7)*, December 12-15, 2007, Kobe

Japan, pp.269-270.

[2] Takayuki Yamada, Shintaro Yamasaki, Shinji Nishiwaki, Kazuhiro Izui and Masataka Yoshimura, Structural Optimization for the Design of Compliant Thermal Actuators Based on the Level Set Method, *8th World Congress on Computational Mechanics (WCCM8)*, June 30- July 4, 2008, Venice, Italy, CD-ROM.

[3] Takayuki Yamada, Shinji Nishiwaki, Kazuhiro Izui and Masataka Yoshimura, A New Level Set-Based Topology Optimization Method Using the Concepts of the Phase Field Method, *10th U.S. National Congress for Computational Mechanics (USNCCM10)*, July 16-19, 2009, Columbus, Ohaio, USA, CD-ROM.

[4] Yutaka Hirano, Takayuki Yamada, Nozomu Kogiso and Shinji Nishiwaki, Level Set-Based Topology Optimization for Thermal Problems Considering Uncertainty, *Proceedings of 9th Japan-Korea Design Engineering Workshop (DEW2009)*, October 26-27, 2009, Okinawa, JAPAN, pp.157-158.

[5] Takayuki Yamada, Kazuhiro Izui and Shinji Nishiwaki, Level-Set Based Topology Optimization for the Design of Capacitive Micromachined Ultrasonic Transducers, *Proceedings of KSME-JSME Joint Symposium 2010 on Computer-Aided Engineering*, March 4-5, 2010,Seoul, Korea, pp.33-34.

[6] Kazuhiro Izui, Yuji Okamoto, Takayuki Yamada and Shinji Nishiwaki, Topology Optimization of Thermal Deformation Control Systems Incorporating Thermoelectric Devices, *Proceedings of KSME-JSME Joint Symposium 2010 on Computer-Aided Engineering*, March 4-5, 2010,Seoul, Korea, pp.29-30.

[7] Takayuki Yamada, Kazuhiro Izui and Shinji Nishiwaki, Topology optimization of Capacitive Micromachined Ultrasonic Transducers Using Level Set Boundary Expressions, *Proceedings of The 2nd International Workshops on Advances in Computational Mechanics*, March 29-31, 2010, Yokohama, Japan, p.62.

[8] Yutaka Hirano, Takayuki Yamada, Nozomu Kogiso, Shinji Nishiwaki and Aturo Iga, Level-Set Based Robust Topology Optimum Design for Coupled Thermal and Structural Problems Using Concept of Phase Field Method, *Proceedings of The 2nd International Workshops on Advances in Computational Mechanics*, March 29-31, 2010, Yokohama, Japan, p.60.

[9] Takayuki Yamada, Kazuhiro Izui and Shinji Nishiwaki, Level Set Method, *9th World Congress on Computational Mechanics and 4th Asian Pacific Congress on Computational Mechanics (WCCM8/APCOM2010)*, July 19- July 23, 2010, Sydney, Australia, CD-ROM.

Domestic Conferences

[1] 杉元宏，山田崇恭，異温度の網のペアを通して誘起される希薄気体の流れ，2007 年春季応用物理関係連合講演会，日本応用物理学会，2007 年 3 月 27 日 - 30 日，東京，日本，28a-P3-23.

[2] 山田崇恭，山崎慎太郎，西脇眞二，泉井一浩，吉村允孝，レベルセット法に基づく構造最適化におけるパラメータ設定の検討，第 20 回計算力学講演会，日本機械学会，2007 年 11 月 26 日 - 28 日，京田辺（京都），日本，pp.677-678.

[3] 山田崇恭，山崎慎太郎，西脇眞二，泉井一浩，吉村允孝，レベルセット法に基づく構造最適化における設計領域境界設定に関する一考察，研究部会連合発表会，日本応用数理学会，2008 年 3 月 8 日 - 9 日，東京，日本.

[4] 山田崇恭，山崎慎太郎，西脇眞二，泉井一浩，吉村允孝，熱アクチュエータのトポロジカルデリバティブを用いたレベルセット法に基づく構造最適化，第 83 期日本機械学会関西支部定時総会講演会，日本機械学会，2008 年 3 月 14 日 - 15 日，大阪，日本，pp.12-10.

[5] 山田崇恭，山崎慎太郎，西脇眞二，泉井一浩，吉村允孝，コンプライアントメカニズムのトポロジカルデリバティブを用いたレベルセット法に基づく構造最適化, 2007 年度精密工学会春季大会，精密工学会，2008 年 3 月 17 日 - 19 日，東京，日本，pp.885-886.

[6] 山田崇恭，山崎慎太郎，西脇眞二，泉井一浩，吉村允孝，熱変形を利用したマイクロアクチュエータのトポロジカルデリバティブを用いたレベルセット法に基づく構造最適化，第 13 回計算工学講演会，日本計算工学会，2008 年 5 月 19 日 - 21 日，仙台，日本, pp.477-480.

[7] 岡本由仁，泉井一浩，山田崇恭，西脇眞二，吉村允孝，John E. Renaud，ペルチェ素子の効率的利用を目的とした熱伝導問題に関するトポロジー最適化，第 13 回計算工学講演会，日本計算工学会，2008 年 5 月 19 日 - 21 日，仙台，日本, pp.443-446.

[8] 山田崇恭，山崎慎太郎，西脇眞二，泉井一浩，吉村允孝，有限設計領域におけるレベルセット法に基づく構造最適化, 第 50 回構造強度に関する講演会，日本航空宇宙学会，2008 年 7 月 29 日-30 日，北九州，日本，pp.4-6.

[9] 岡本由仁，泉井一浩，山田崇恭，伊賀淳郎，西脇眞二，吉村允孝，John E. Renaud，熱電冷却モジュールのトポロジー最適化，2008 年度関西地方学術講演会，精密工学会，2008 年 7 月 29 日 - 30 日，大阪，日本，pp.99-100.

[10] 山田崇恭，竹澤晃弘，西脇眞二，泉井一浩，吉村允孝，Phase-field 理論に基づく領域形状・形態最適化問題の一解法, 日本応用数理学会 2008 年度年会，日本応用数理学会，2008 年 9 月 17 日 - 19 日，千葉，日本，pp.299-300.

[11] 山田崇恭，山崎慎太郎，西脇眞二，泉井一浩，吉村允孝，車谷麻緒，寺田賢二郎，有限被覆法を用いたレベルセット法に基づく構造最適化, 第 18 回設計工学システム部門講演会，日本機械学会，2008 年 9 月 25 日 - 27 日，京都，日本，pp.394-396.

[12] 山崎慎太郎，山田崇恭，西脇眞二，泉井一浩，吉村允孝，構造最適化に基づくデ

ザイン知識の獲得に関する一考察, 第18回設計工学システム部門講演会，日本機械学会，2008年9月25日‐27日，京都，日本，pp.521-524.

[13] 横田清志，山田崇恭，泉井一浩，西脇眞二，吉村允孝，ユニバーサルデザインを目指したコンプライアントメカニズムの創生的設計手法の構築, 第18回設計工学システム部門講演会，日本機械学会，2008年9月25日‐27日，京都，日本，pp.525-528.

[14] 山田崇恭，竹澤晃弘，西脇眞二，泉井一浩，吉村允孝，Phase-field 法に基づく機械構造物の構造最適化, 第21回計算力学講演会，日本機械学会，2008年11月1日‐3日，沖縄，日本, pp.223-224.

[15] 岡本由仁，泉井一浩，山田崇恭，伊賀淳郎，西脇眞二，吉村允孝，熱電モジュールを利用したマルチフィジックス問題に関するトポロジー最適化, 第21回計算力学講演会，日本機械学会，2008年11月1日‐3日，沖縄，日本， pp.231-232.

[16] 加藤峰教，山田崇恭，永井学志，西脇眞二，磁歪アクチュエータの構造最適化に関する基礎的検討, 第21回計算力学講演会，日本機械学会，2008年11月1日‐3日，沖縄，日本, pp.508-509.

[17] 山田崇恭，竹澤晃弘，西脇眞二，泉井一浩，吉村允孝，レベルセットモデルを用いた Phase-field 法に基づく機械構造物の構造最適化, 最適化シンポジウム 2008（OPTIS2008），日本機械学会，2008年11月27日‐28日，東京，日本，pp.225-228.

[18] 山田崇恭，竹澤晃弘，西脇眞二，泉井一浩，吉村允孝，構造最適化手法に基づくエコデザイン, エコデザイン 2008 ジャパンシンポジウム，エコデザイン学会連合，2008年12月11日‐12日， 東京， 日本， A23-2.

[19] 山田崇恭，西脇眞二，泉井一浩，吉村允孝，レベルセット法に基づく設計変数依存型境界条件を含む形態最適化問題の解法, 研究部会連合発表会，日本応用数理学会，2009年3月7日‐8日，京都，日本.

[20] 山田崇恭，西脇眞二，泉井一浩，吉村允孝，レベルセット法による形状表現を用いた放熱器のトポロジー最適化, 2008 年度精密工学会春季大会， 精密工学会，2009 年 3 月 11 日 - 13 日， 東京， 日本， pp.271-272.

[21] 山田崇恭，西脇眞二，泉井一浩，吉村允孝，レベルセット法に基づくコンプライアントメカニズムの最適形態創成設計法，第 84 期日本機械学会関西支部定時総会講演会，日本機械学会，2009 年 3 月 16 日 - 17 日，大阪，日本，604.

[22] 花谷大輔，山田崇恭，西脇眞二，泉井一浩，吉村允孝，レベルセット法に基づくトポロジー最適化における幾何学的制約に関する一考察，第 84 期日本機械学会関西支部定時総会講演会，日本機械学会，2009 年 3 月 16 日-17 日，大阪，日本，605.

[23] 平野佑享，山田崇恭，小木曽望，西脇眞二，泉井一浩，吉村允孝，レベルセット法を用いた信頼性に基づくトポロジー最適設計，第 84 期日本機械学会関西支部定時総会講演会，日本機械学会，2009 年 3 月 16 日 - 17 日，大阪，日本，606.

[24] 山田崇恭，西脇眞二，泉井一浩，吉村允孝，レベルセットモデルを用いた平均温度最小化問題のトポロジー最適化，第 14 回計算工学講演会， 日本計算工学会，2009 年 5 月 12 日 - 14 日， 東京， 日本， pp.63-66.

[25] 平野佑享，山田崇恭，小木曽望，西脇眞二，単一ループの信頼性解析を用いたレベルセット法に基づくトポロジー最適化，第 14 回計算工学講演会，日本計算工学会，2009 年 5 月 12 日 - 14 日， 東京，日本, pp.67-70.

[26] 岡本由仁，泉井一浩，山田崇恭，西脇眞二，吉村允孝，熱電効果を利用した熱アクチュエータの創成的最適設計, 2009 年度関西地方定期学術講演会，精密工学会，2009 年 5 月 13 日，大阪，日本.

[27] 山田崇恭，西脇眞二，泉井一浩，吉村允孝，山本崇史，丸山新一，レベルセット法に基づく最適設計法のボデー構造設計への展開，2009 年春季学術講演会，自動車技術会，2009 年 5 月 20 日 - 22 日，神奈川，日本，No.51-09，pp.11-14.

[28] 山田崇恭，西脇眞二，泉井一浩，吉村允孝，剛性最大化を目的としたレベルセット法に基づくトポロジー最適化，第 51 回構造強度に関する講演会，日本航空宇宙学会，2009 年 7 月 22 日 - 24 日，和歌山，日本, pp.1-3.

[29] 山田崇恭，西脇眞二，泉井一浩，固有振動数最大化問題に対するレベルセット法に基づくトポロジー最適化，第 53 回宇宙科学技術連合講演会， 日本航空宇宙学会，2009 年 9 月 9 日 - 11 日，京都，日本， pp.1499-1502.

[30] 岡本由仁，山田崇恭，泉井一浩，西脇眞二，熱電アクチュエータの設計に対するレベルセット法に基づくトポロジー最適化，2009 年度秋季大会，精密工学会，2009 年 9 月 10 日 - 12 日， 神戸， 日本， pp.871-872.

[31] 山田崇恭，西脇眞二，泉井一浩，固有値問題におけるレベルセット法による形状表現を用いたトポロジー最適化，日本応用数理学会 2009 年度年会，日本応用数理学会，2009 年 9 月 28 日 - 30 日，大阪，日本，pp.315-316.

[32] 山田崇恭，西脇眞二，泉井一浩，振動特性を設計目標とする機械構造物のレベルセット法に基づくトポロジー最適化，第 22 回計算力学講演会， 日本機械学会, 2009 年 10 月 10 日 - 12 日， 石川， 日本， pp.145-146.

[33] 真鍋匡利，山田崇恭，西脇眞二，泉井一浩，粒子法を用いたレベルセット法に基づくトポロジー最適化，第 22 回計算力学講演会，日本機械学会，2009 年 10 月 10 日 - 12 日，石川，日本，pp.402-403.

[34] 岡本由仁，山田崇恭，泉井一浩，西脇眞二，レベルセット法に基づく熱電効果を考慮した熱弾性問題のトポロジー最適化，第 22 回計算力学講演会，日本機械学会, 2009 年 10 月 10 日 - 12 日，石川， 日本， pp.400-401.

[35] 平野佑享，山田崇恭，小木曽望，西脇眞二，不確定性を考慮した熱問題に対するレベルセット法に基づくトポロジー最適化，第 22 回計算力学講演会，日本機械学会，2009 年 10 月 10 日 - 12 日，石川，日本， pp.141-142.

[36] 加藤峰教，山田崇恭，永井学志，西脇眞二，レベルセット法に基づく磁歪アクチュエータ構造設計のためのトポロジー最適化，第 22 回計算力学講演会，日本機械学会，2009 年 10 月 10 日 - 12 日，石川，日本，pp.143-144.

[37] 山田崇恭，西脇眞二，泉井一浩，レベルセット法に基づく機械構造物の最適形態創成設計法，第 19 回設計工学システム部門講演会，日本機械学会，2009 年 10 月 28 日 - 30 日，沖縄，日本，pp.128-130.

[38] 岡本由仁，泉井一浩，山田崇恭，西脇眞二，熱電効果を利用した柔軟構造物のレベルセット法に基づく最適形状創成設計法，第 19 回設計工学システム部門講演会，日本機械学会，2009 年 10 月 28 日 - 30 日，沖縄，日本，pp.145-150.

[39] 平野佑享，山田崇恭，小木曽望，西脇眞二，熱拡散問題に対するレベルセット法を用いた信頼性に基づくトポロジー最適設計，第 19 回設計工学システム部門講演会，日本機械学会，2009 年 10 月 28 日 - 30 日，沖縄，日本，pp.151-154.

[40] 西脇眞二，山田崇恭，トポロジー最適化の最前線 - 基本的な考え方と応用事例 -，コロキウム構造形態の解析と創生 2009，日本建築学会，2009 年 11 月 12 日－13 日，東京，日本，pp.5-12.

[41] 真鍋匡利，山田崇恭，泉井一浩，西脇眞二，粒子法を用いたレベルセット法に基づく幾何学的非線形性を伴う構造物のトポロジー最適化，コロキウム構造形態の解析と創生 2009，日本建築学会，2009 年 11 月 12 日 - 13 日，東京，日本，pp.115-120.

[42] 山田崇恭，泉井一浩，西脇眞二，固有振動数最大化を目的としたレベルセット法に基づくトポロジー最適化法，コロキウム構造形態の解析と創生 2009，日本建築学会，2009 年 11 月 12 日 - 13 日，東京，日本，pp.133-136.

[43] 岩井裕，黒柳篤史，齋藤元浩，吉田英生，山田崇恭，西脇眞二，トポロジー最適化手法に基づく SOFC 電極-電解質界面の形状制御，第 47 回日本伝熱シンポジウム，日本伝熱学会，2010 年 5 月 26 日 - 28 日，札幌，日本.

[44] 山田崇恭，泉井一浩，西脇眞二，不知加寿子，Alejandoro R. Diaz，野村壮史，レベルセット法に基づくフォトニックバンドギャップ構造のトポロジー最適化，第15回計算工学講演会，日本計算工学会，2010年5月26日 - 28日，福岡，日本，pp.1085-1088.

[45] 真鍋匡利，山田崇恭，泉井一浩，西脇眞二，車谷麻緒，寺田賢二郎，有限被覆法を用いたレベルセット法に基づくトポロジー最適化，第15回計算工学講演会，日本計算工学会，2010年5月26日 - 28日，福岡，日本， pp.1089-1092.

[46] Lim Yi Kang，山田崇恭，泉井一浩，西脇眞二，レベルセット法に基づくピエゾ素子のトポロジー最適化，第15回計算工学講演会，日本計算工学会，2010年5月26日 - 28日，福岡，日本， pp.1081-1084.

Index